Linear assistance filter design for electric power steering systems with improved delay margin

Ali Diab, Giorgio Valmorbida, William Pasillas-Lépine

INTERNATIONAL JOURNAL OF CONTROL
https://doi.org/10.1080/00207179.2023.2201648

Taylor & Francis
Taylor & Francis Group

Linear assistance filter design for electric power steering systems with improved delay margin

Ali Diab [a,b], Giorgio Valmorbida[a,b] and William Pasillas-Lépine[a]

[a]Laboratoire des signaux et systèmes, CNRS, CentraleSupélec, Université Paris-Saclay, Gif-sur-Yvette, France; [b]Projet Team DISCO, Inria, Paris, France

ABSTRACT

This paper studies the achievable delay margin using lead-lag filter structures for Electric Power Steering systems. We propose an approximation of the delay margin as an explicit function of filter parameters. Our results provide useful guidelines for adjusting the different filter parameters to ensure system stability in the presence of a time delay. Simulation results show that the proposed filter structures can attenuate vibrations and improve steering feel and road feel. As a consequence, the influence of the delay on the system can be minimised with little performance degradation.

ARTICLE HISTORY
Received 12 January 2022
Accepted 23 March 2023

KEYWORDS
Time-delay systems; electric power steering; delay margin; linear filters; automotive control; steering and road feel

1. Introduction

Thanks to technological advances, Electric Power Steering (EPS) is replacing hydraulic power steering. Among the advantages of EPS, we can list: variable assistance gains, engine independence, and fuel economy (Y. Li et al., 2018). However, the design of control laws for EPS requires further robustness, in particular, to cope with computational and measurement delays.

In this context, control laws were proposed to increase robustness and improve performance. In D. Lee, Kim, et al. (2018), the robustness of a linearised system is studied by bounding the gain and phase margins, and an optimisation-based computation of poles and zeros of a lead-lag compensator is proposed. In Zaremba et al. (1997), the bandwidth is considered in an optimisation-based control law design to find a balance between useful information transmitted to the driver and disturbances. In Zaremba et al. (1998), an objective function allows to adjust the information transmitted from the road to the driver. As performance indicators in EPS, we can consider the driver's steering feel and road feel (Marouf et al., 2012). Steering feel is related to how the steering torque is transmitted to the driver and how the vehicle responds to steering wheel manoeuvres – see, *e.g.* Zaremba et al. (1998) and Y. Li et al. (2018). In M. H. Lee et al. (2005), a torque map based on a third-order polynomial was proposed to improve the steering stiffness and return-to-centre performance of the steering system. Moreover, to achieve a satisfactory road feel, the driver must receive appropriate feedback from the forces generated by the contact between the tire and the road – see, e.g. Sugitani et al. (1997) and Marouf et al. (2012). In D. Lee et al. (2021), the steering feel design problem is distinguished from the system stability problem while tuning the filter parameters. In those papers, however, the impact of the delays on the stability of the system has not been considered explicitly. To fill this gap, in this paper we study the delay margin of the main feedback loop associated with EPS systems. These delays are *internal* since they are generated by the processing of local measurements and by the time required to compute the control input in real time. In contrast to the communication and network transmission delays, the internal delays are generally small. Moreover, even when they are time-varying, these delays remain *bounded* (X. Li et al., 2009). As a consequence, the apparent delays can still be made constant by buffering data up to a certain (known) worst-case maximum delay, using a timestamp – see, e.g. D. Lee and Spong (2006). On the other hand, in Baek and Kang (2020), delays are introduced in the control law design to obtain a given closed-loop convergence rate despite disturbances and unmodelled dynamics.

Compared to other design specifications, the delay margin is particularly important for EPS since, for these systems, feedback loop delays appear as the main destabilising term. Indeed, for the delay-free dynamics, a proportional assistance scheme results in a stable closed-loop for any control gain. In contrast, a delay in the feedback loop can destabilise the system unless a filtering term is included to increase the delay margin of the EPS system. For this reason, the feedback loop analysed in our paper consists of a stable second-order system in feedback with different filter structures and is subject to delays. The considered second-order system represents the pinion subsystem dynamics, which is the EPS subset that is most sensitive to delays. There exists already a large literature on filter design for EPS systems, where optimal filter parameters are proposed for a fixed filter structure. However, this is usually done without accounting for the delays in the feedback loop – see, e.g. Zaremba et al. (1998) and D. Lee, Kim, et al. (2018). In addition, most existing results in this area aim to design filters by minimising an objective function. To achieve the performance requirements of the steering

CONTACT Ali Diab ali.diab@centralesupelec.fr, alikdiab@outlook.com Laboratoire des signaux et systèmes, CNRS, CentraleSupélec, Université Paris-Saclay, Gif-sur-Yvette 91190, France

system, they impose constraints on the filter gain, such as the phase margin and the location of poles and zeros, in general leading to high-order filters. Such high-order filters are prone to undesirable effects on the system. Moreover, the controller synthesis accounting for these constraints imposes the resolution of a complex nonlinear optimisation problem. In contrast, our results aim to maximise the delay margin using low-order filters, which lead to analytical bounds for the delay margin and preserve the steering system performance.

In this paper, for several of the previously considered filter structures, we carry out the stability analysis, which provides delay margin approximations in an explicit form as a function of the filter parameters. Importantly, we have focused on filter structures for which an analytical bound for the delay margin, or the delay margin itself, is explicitly obtained. For the Proportional-Derivative (PD) filter, a lower bound of the derivative gain parameter is obtained, providing explicit lower bounds of the achievable delay margin and an asymptotic value of the optimal filter parameter. The main benefit of the presented results is that these explicit forms provide guidance for the design of filters that take into account delay margin requirements. In the case of the proportional-derivative filter, the obtained bounds are related to the results in D. Ma et al. (2019), where the derivative gain maximising the delay margin has been analysed for unstable systems.

The paper is organised as follows: Section 2 presents the EPS system model and introduces the considered filter structures. In Section 3, explicit equations of the delay margin are presented with the different filter structures and present the main result at Theorems 3.4 and 3.5. The simulation section compares the performance of the filters for selected filter parameters; a comparison with a state-of-the-art controller is also included. The mathematical proofs of the proposed results are given in the Appendix.

2. EPS model and problem statement

We consider the following model for the EPS dynamics

$$\begin{aligned} J_w\ddot{\theta}_w &= k_s(\theta_p - \theta_w) - \sigma_w\dot{\theta}_w + T_d \\ J_p\ddot{\theta}_p &= k_s(\theta_w - \theta_p) - \sigma_p\dot{\theta}_p - T_r + T_a, \end{aligned} \tag{1}$$

where θ_w and θ_p are, respectively, the steering wheel angle and the pinion angular position. The road reaction torque T_r and the driver steering torque T_d are inputs of the system. The stiffness k_s of the torque sensor provides

$$T_s = k_s(\theta_w - \theta_p),$$

the torque that appears in (1). Figure 1 shows the mechanical model of an EPS system. The remaining model parameters and their numerical values are reported in Table 1, in Section 4.

Figure 2 illustrates the control flow chart of the proposed control scheme of an electric power steering system. The input u_1 is the total torque applied to the pinion subsystem, which is equal to the sum of the reaction torque associated with the road torque T_r and the torque generated by the mechanical link between the steering wheel and the pinion subsystems. In a general form, we use the assist torque map $\kappa : \mathbb{R} \to \mathbb{R}$,

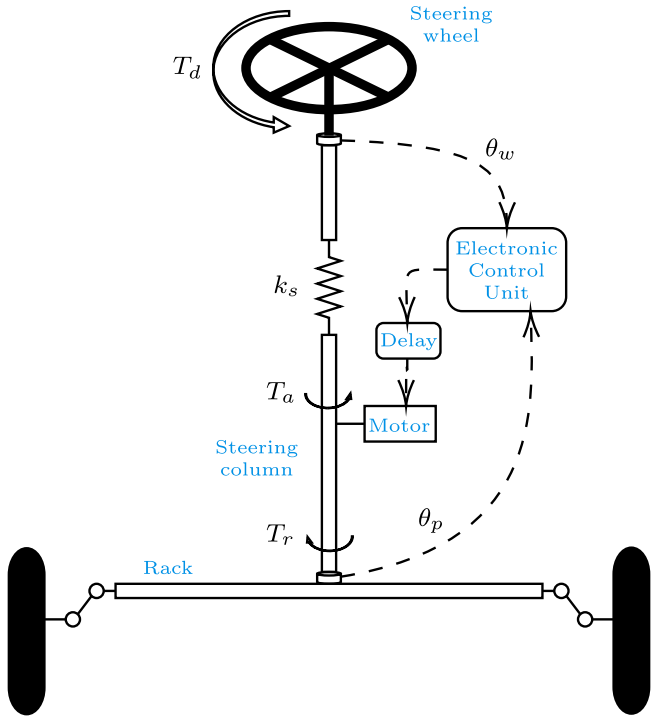

Figure 1. Scheme of the EPS system.

Table 1. EPS parameters – see D. Lee, Kim, et al. (2018).

Symbol	Description	Value
k_s	torque sensor stiffness	143.24 Nm/rad
J_w	steering wheel moment of inertia	0.044 Kg.m^2
σ_w	steering wheel viscous damping	0.25 Nm.s/rad
J_p	pinion moment of inertia	0.11 Kg.m^2
σ_p	pinion viscous damping	1.35 Nm.s/rad
K	assist gain	35

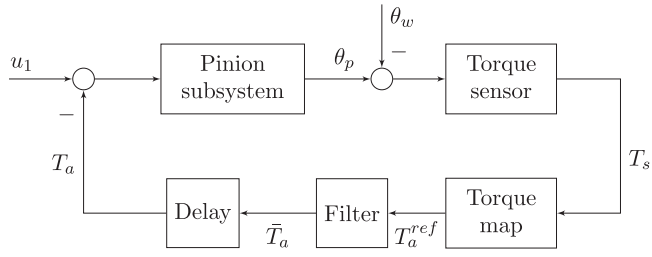

Figure 2. Block diagram of the EPS pinion subsystem.

and functions $f : \mathbb{R}^n \times \mathbb{R} \to \mathbb{R}^n, g : \mathbb{R}^n \times \mathbb{R} \to \mathbb{R}$ to design the assist torque $\bar{T}_a$ as follows

$$\begin{aligned} T_a^{ref}(t) &= \kappa(\theta_w(t) - \theta_p(t))T_s(t) \\ \dot{x}(t) &= f(x(t), T_a^{ref}(t)) \\ \bar{T}_a(t) &= g(x(t), T_a^{ref}(t)) \\ T_a(t) &= \bar{T}_a(t-\tau), \end{aligned} \tag{2}$$

where x is the state variable of a filter and T_a^{ref} is a signal defining a reference for the assist torque (D. Lee, Yi, et al., 2018). The

actual assist torque T_a corresponds to the output of the filter $\bar{T}_a$ delayed by τ seconds.

Whenever the assist torque map κ is constant, that is $\kappa(\theta_w - \theta_p) = K$, we say $K > 0$ is the *assist gain* – see, e.g. Yamamoto et al. (2019). If, moreover, f and g are linear mappings, system (2) is a linear system and it can be expressed in the Laplace domain as

$$T_a(s) = Kk_s\, \mathrm{e}^{-\tau s} C(s)(\theta_w(s) - \theta_p(s)), \tag{3}$$

with C the Laplace transform of a linear filter. The parameter K is determined by a steady-state analysis of the system. In steady state, K is proportional to the ratio between the road torque and the driver torque. For a given road condition, if the value of K is small, the force applied by the driver should be higher to compensate for the road reaction forces. Therefore, the value of K is chosen to limit the forces the driver must apply, which guarantees a certain level of comfort from the assisted system.

The resulting linear system (1)–(3) is represented in Figure 3 with its intermediate signals as in (2). In this paper, we study the feedback loop introduced by the delayed control law in the pinion subsystem. Namely, we focus on the subsystem depicted in Figure 4. More precisely, we study the stability of the transfer function between u_1 and θ_p given by

$$G(s) = \frac{1}{Kk_s}\left(\frac{\frac{Kk_s}{J_p s^2+\sigma_p s+k_s}}{1+\frac{Kk_s}{J_p s^2+\sigma_p s+k_s}C(s)\,\mathrm{e}^{-\tau s}}\right).$$

Defining $\omega_0 = \sqrt{\frac{k_s}{J_p}}$ and $\zeta = \frac{\sigma_p}{2\sqrt{k_s J_p}}$, and introducing $\bar{s} = \frac{s}{\omega_0}$ and $\bar{\tau} = \tau\omega_0$, we have that the above transfer function is expressed as

$$G(\bar{s}) = \frac{1}{Kk_s}\left(\frac{P(\bar{s})}{1+P(\bar{s})C(\bar{s})\,\mathrm{e}^{-\bar{\tau}\bar{s}}}\right), \tag{4}$$

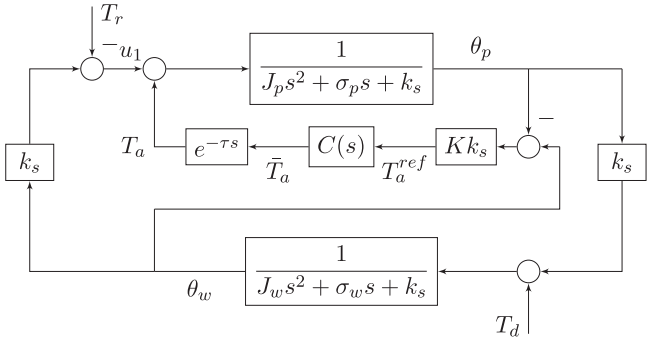

Figure 3. Block diagram of the EPS system.

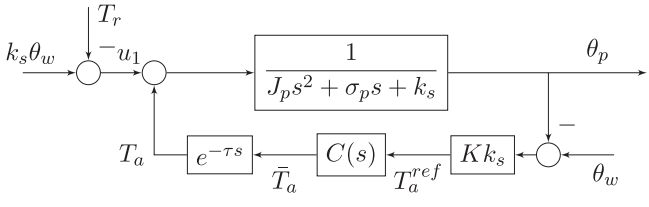

Figure 4. Block diagram of the pinion subsystem.

Table 2. Filter structures.

$C_1(s)$	$C_2(s)$	$C_3(s)$	$C_4(s)$	$C_5(s)$
1	$\frac{s}{\omega_a}+1$	$\frac{\frac{s}{\omega_a}+1}{\frac{s}{\omega_b}+1}$	$\frac{s^2+2\zeta_f s+1}{\left(\frac{s}{\omega_p}+1\right)\left(\frac{s}{\omega_q}+1\right)}$	$\frac{\left(s^2+2\zeta_f s+1\right)\left(\frac{s}{\omega_a}+1\right)}{\left(\frac{s}{\omega_p}+1\right)\left(\frac{s}{\omega_q}+1\right)}$

with

$$P(\bar{s}) = \frac{K}{\bar{s}^2+2\zeta\bar{s}+1}. \tag{5}$$

For a given control law $C(\bar{s})$, the *delay margin* (Middleton & Miller, 2007) of the pinion subsystem (4) is defined by

$$\Delta\bar{\tau} = \sup\{\bar{\tau} \geq 0 : G(\bar{s}) \text{ is stable } \forall\, \tau \leq \bar{\tau}\}.$$

Remark 2.1: *Since the actual $\bar{s}$ is a scaling of s, the delay margin is given by $\Delta\tau = \Delta\bar{\tau}/\omega_0$ in the above expressions. To keep the notation simple, we will use s instead of $\bar{s}$ in the rest of the paper. Thus, when using $G(s)$ and $P(s)$, we refer to (4) and (5), respectively.*

The goal of this paper is to compute delay margin estimates of the feedback loop for five different structures of the linear filter C. These structures are partially inspired by approaches from the literature, for instance those in Zaremba et al. (1997) and D. Lee, Kim, et al. (2018), where fixed-structure compensators have been proposed to stabilise the system and minimise torque vibrations. The suggested structures combine traditional lead-lag compensators. In particular, we will study the structures of C presented in Table 2: C_1 is the filter without any compensation, C_2 is an ideal PD filter where ω_a is the inverse of the derivative coefficient, while C_3 adds extra dynamics to the PD filter to make it proper and to reduce the high-frequency gain (D. Lee, Kim, et al., 2018). The filter C_4 is defined to compensate for the dynamics of the second-order system and impose a second-order behaviour with two real poles (Zaremba et al., 1997) to provide an improved delay margin. Finally, to prevent the performance degradation of C_4, the filter C_5 combines C_4 and C_2. For an EPS system without delay, when the system disturbances are not considered, the stability of the feedback loop can be achieved without using a filter, taking $C_1(s) = 1$. However, when time delays are included in the feedback loop, we propose to introduce a cascade of N lead-lag filters, where N is determined by the desired robustness level of the system. In this paper, we focus on filters with a limited order to allow an analytical computation of the delay margin or a lower bound of it as a function of the filter parameters. Moreover, in applications, low-order filters are often preferred because of their simplicity of implementation (Chen et al., 2008). Note that the filter parameters are usually chosen based on the parameters of the EPS system, namely the assist gain K and the damping coefficient ζ. Below, we will omit the dependence of the filter parameters on the EPS system parameters, hence, when there is no ambiguity, we will write ω_i instead of $\omega_i(K,\zeta)$, for $i \in \{a,b,p,q\}$.

3. Robustness with respect to delays

In this section, we study the effect of the filter parameters on the delay margin of the EPS system for the different filter structures

considered in Table 2. A separate study of each filter is detailed below.

3.1 Delay margin with C_1

We start analysing the robustness of the system without any compensation filter, that is for $C(s) = 1$. The following result is well known. Its proof can be found in Niculescu (2001, Proposition 4.20 and Proposition 4.22).

Proposition 3.1: *Let G be given by (4), with P given by (5), where $K > 0$ and $\zeta > 0$.*

(i) *The delay margin of G with $C = C_1$ is infinite if and only if*

$$K \leq 1 \quad \text{and} \quad \zeta^2 > \frac{1 - \sqrt{1 - K^2}}{2}; \tag{6}$$

(ii) *If (6) does not hold, then the delay margin $\Delta\bar{\tau}$ is given by*

$$\Delta\bar{\tau} = \begin{cases} \dfrac{\tan^{-1}\frac{2\zeta\hat{\omega}_c}{\hat{\omega}_c^2 - 1}}{\hat{\omega}_c}, & \text{if } \hat{\omega}_c > 1, \\ \dfrac{\pi}{2}, & \text{if } \hat{\omega}_c = 1, \\ \dfrac{-\tan^{-1}\frac{2\zeta\hat{\omega}_c}{1-\hat{\omega}_c^2} + \pi}{\hat{\omega}_c}, & \text{if } \hat{\omega}_c < 1, \end{cases}$$

where

$$\hat{\omega}_c = \sqrt{\frac{2 - 4\zeta^2 + \sqrt{(2-4\zeta^2)^2 - 4 + 4K^2}}{2}}. \tag{7}$$

The following corollary gives an explicit upper bound for the delay margin in the case of Item (ii) of Proposition 3.1. This upper bound explicitly shows the dependence of the delay margin in terms of the assist gain K, which is the main parameter that limits the delay margin.

Corollary 3.2: *If (6) does not hold, the delay margin is a strictly decreasing function of K and is upper-bounded by*

$$\Delta\bar{\tau} \leq \begin{cases} \dfrac{4\zeta}{-4\zeta^2 + \sqrt{(2-4\zeta^2)^2 - 4 + 4K^2}}, & \text{if } \hat{\omega}_c > 1, \\ \dfrac{\pi}{2}, & \text{if } \hat{\omega}_c = 1, \\ \dfrac{\sqrt{2}\pi}{\sqrt{2 - 4\zeta^2 + \sqrt{(2-4\zeta^2)^2 - 4 + 4K^2}}}, & \text{if } \hat{\omega}_c < 1. \end{cases} \tag{8}$$

The proof of the above corollary relies on Lemma A.1 in the Appendix.

Remark 3.1: *From the expressions (7) and (8), for a fixed ζ, there exist $K_0(\zeta)$ and $\alpha(\zeta)$ such that, for all $K \geq K_0$, we have $\Delta\bar{\tau} \leq \alpha/K$. From this upper bound we can thus observe that a large value of the assist gain K results in a small delay margin. Moreover, from (6), for $K \leq 1$ there always exist a value of ζ such that the delay margin is infinite. Since ζ depends only on the system parameters σ_p, k_s, and J_p, and since K is a design parameter, using (6) we can always obtain an infinite delay margin with*

$$0 < K < \begin{cases} 2\zeta\sqrt{1-\zeta^2}, & \text{if } 0 < \zeta \leq \sqrt{\frac{1}{2}}, \\ 1, & \text{otherwise.} \end{cases}$$

One should stress that, even if theoretically the delay margin can be increased by decreasing the value of K, in practice this cannot be done since the parameter K describes the amount of assistance provided to the driver.

3.2 Improving the delay margin with the lead filter C_2

In this section, we consider the second-order stable system in (5) in feedback with the filter

$$C_2(s) = \frac{s}{\omega_a} + 1. \tag{9}$$

The proposition below characterises the delay margin for system (4) with $C = C_2$ in terms of the parameter ω_a.

Proposition 3.3: *Let G be given by (4), with P given by (5), where $K > 0$ and $\zeta > 0$.*

(i) *The delay margin of G with $C = C_2$ is infinite if and only if*

$$K \leq 1 \quad \text{and} \quad \frac{1}{\omega_a^2} < \frac{2\sqrt{1-K^2} + 4\zeta^2 - 2}{K^2}. \tag{10}$$

Moreover, there exists a value of ω_a such that (10) holds if and only if (6) holds;

(ii) *If (10) does not hold, then the delay margin $\Delta\bar{\tau}(\omega_a)$ as a function of ω_a is given by*

$$\Delta\bar{\tau}(\omega_a) = \begin{cases} \dfrac{\tan^{-1}\frac{\tilde{\omega}_c(\omega_a)}{\omega_a} + \tan^{-1}\frac{2\zeta\tilde{\omega}_c(\omega_a)}{\tilde{\omega}_c^2(\omega_a)-1}}{\tilde{\omega}_c(\omega_a)}, & \text{if } \tilde{\omega}_c(\omega_a) > 1, \\ \dfrac{\pi}{2} + \tan^{-1}\dfrac{1}{\omega_a}, & \text{if } \tilde{\omega}_c(\omega_a) = 1, \\ \dfrac{\tan^{-1}\frac{\tilde{\omega}_c(\omega_a)}{\omega_a} - \tan^{-1}\frac{2\zeta\tilde{\omega}_c(\omega_a)}{1-\tilde{\omega}_c^2(\omega_a)} + \pi}{\tilde{\omega}_c(\omega_a)}, & \text{if } \tilde{\omega}_c(\omega_a) < 1, \end{cases} \tag{11}$$

where

$$\tilde{\omega}_c(\omega_a) = \sqrt{\frac{\frac{K^2}{\omega_a^2} + 2 - 4\zeta^2 + \sqrt{\left(\frac{K^2}{\omega_a^2} + 2 - 4\zeta^2\right)^2 - 4 + 4K^2}}{2}}. \tag{12}$$

The proof of the above proposition is given in the Appendix. Note that when (6) is satisfied the delay margin of G with C_1 is infinite, it is therefore useless to add a lead filter C_2 in this case

to increase the delay margin. Moreover, when (6) is satisfied, condition (10) can also be satisfied provided a large value of the parameter ω_a is used, and thus an infinite delay margin can be achieved. For this reason, the next theorem is restricted to the case where (6) is not satisfied. In this case, we also have that (12) is strictly positive.

Determining from (11) an explicit expression for the value of the parameter ω_a that maximises the delay margin can be difficult. Nevertheless, we can obtain upper bounds for the values of ω_a that maximise the delay margin as in the following theorem.

Theorem 3.4: *If (6) does not hold true, the maximum delay margin of G with $K>0$, $\zeta>0$, and $C=C_2$, is attained at $\omega_a=\omega_a^*$ satisfying*

$$\omega_a^*(\zeta,K) < \bar{\omega}_a^*(\zeta,K),$$

where the upper bound $\bar{\omega}_a^*(\zeta,K)$ is expressed as

(I) $\sqrt[4]{\frac{1}{5}(4+8K^2+4c_1^2+64c_2^4)}$, *if $K>1$ and $K\geq 2\zeta$,*

(II) $\sqrt[4]{\frac{1}{5}(4+8K^2c_0+4c_1^2c_0^2+64c_2^4c_0^4)}$, *if $K\leq 1$ and $K\geq 2\zeta$,*

(III) $\sqrt[4]{4+4K^2+2(c_1^2+c_3^2)+32(c_2^4+c_4^4)}$, *if $K>1$ and $K<2\zeta$,*

(IV) $\sqrt[4]{4+4K^2c_0+2(c_1^2+c_3^2)c_0^2+32(c_2^4+c_4^4)c_0^4}$, *if $K\leq 1$ and $2\zeta\sqrt{1-\zeta^2}<K<2\zeta$,*

where $c_0=\frac{2-4\zeta^2}{\sqrt{(2-4\zeta^2)^2-4+4K^2}}$, $c_1=\frac{4\zeta K^2\hat{\omega}_c^2}{(\hat{\omega}_c^2-1)^2}$, $c_2=\frac{4\zeta K^2}{(\hat{\omega}_c^2-1)^2}$, $c_3=\frac{K^2\pi}{\hat{\omega}_c}$, and $c_4=\frac{K^2\pi}{\hat{\omega}_c^3}$, with $\hat{\omega}_c$ as in (7).

First note that the four cases of Theorem 3.4, depicted in Figure 5, correspond to the set of values for K and ζ that do not satisfy (6). The proof of the above theorem is detailed in the Appendix. It is divided into three steps. The first step concerns the four cases and shows that there exists a maximum value for the delay margin as a function of the parameter ω_a. The second step details how the bounds are obtained for cases I and II, while the final step shows how to obtain the bounds for cases III and IV.

For a fixed value of K and for several values of ζ, the upper bounds $\bar{\omega}_a^*$ (given by Theorem 3.4) are compared in Figure 6 to the filter parameters ω_a^* that maximise the delay margin (obtained by computing the optimal value of the delay margin with a line search). The curves for the delay margin as a function of ω_a were plotted from relations (11)-(12). One can observe from this figure that the sharpness of the obtained bound depends on the value of ζ.

Using Proposition 3.3, we can compute the delay margin for each fixed value of ω_a. The value of ω_a that provides the maximal delay margin is denoted $\omega_a^*(K,\zeta)$. The uniqueness of this optimum, for large values of K, is proven in Theorem 3.5 below. Moreover, even if an analytical expression of ω_a^* is not available, the following result shows that the value of ω_a^* does not depend on ζ, and it gives an asymptotic estimation of its value, for large values of K.

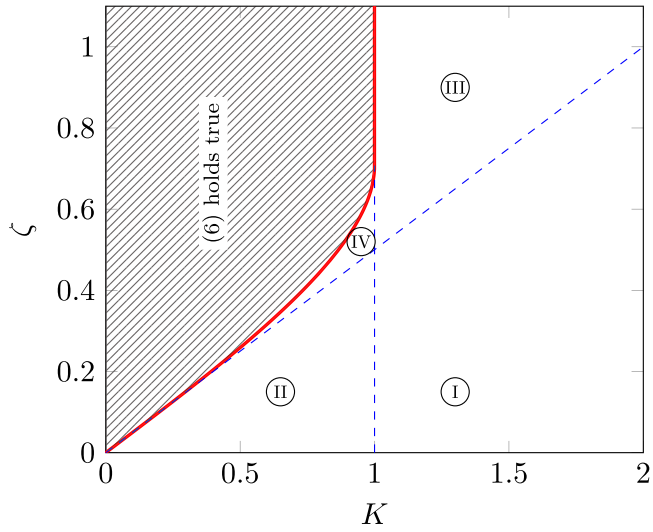

Figure 5. The four different cases where (6) does not hold true.

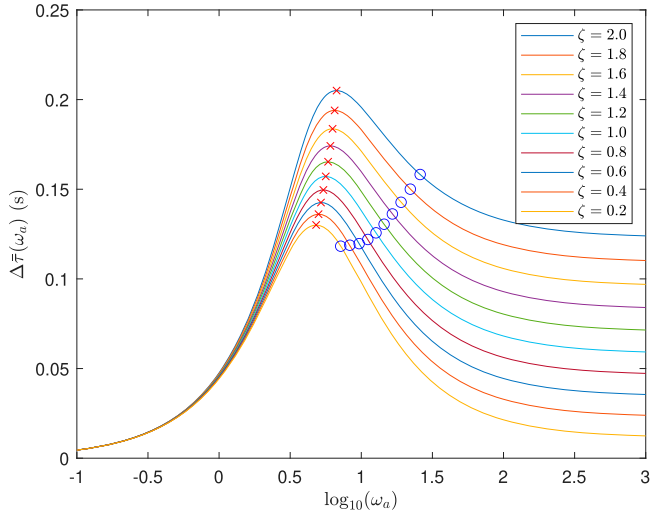

Figure 6. Delay margin as a function of ω_a as in (11)–(12), for $K=35$ and for different values of ζ: The crosses in red correspond to the optimal delay margin for each value of ω_a^*, while the blue circles provide the upper bound $\bar{\omega}_a^*$ and the corresponding delay margin using (11)–(12) and the bounds of ω_a^*, given by Theorem 3.4.

Theorem 3.5: *For any fixed value of $\zeta>0$, we have*

$$\lim_{K\to+\infty}\frac{\omega_a^*(K,\zeta)}{\alpha\sqrt{K}}=1,$$

where $\alpha>0$ is the unique solution of the implicit equation

$$\frac{\beta(\alpha)}{\alpha\gamma(\alpha)}\tan^{-1}\frac{\beta(\alpha)}{\alpha}-\frac{\beta^2(\alpha)+\frac{\beta^2(\alpha)}{\alpha^2\gamma(\alpha)}}{1+\frac{\beta^2(\alpha)}{\alpha^2}}=0, \qquad (13)$$

with $\beta(\alpha)=\sqrt{\frac{\frac{1}{\alpha^2}+\sqrt{\frac{1}{\alpha^4}+4}}{2}}$ and $\gamma(\alpha)=\sqrt{\frac{1}{\alpha^4}+4}$.

The proof of the above theorem is detailed in the Appendix.

Remark 3.2: *The nonlinear equation (13) can be solved numerically, and it gives an approximate value $\alpha\approx 0.7820$.*

Using Item (ii) of Proposition 3.3 and the lower bounds for $\tan^{-1}$ from Mortici and Srivastava (2014, Equation (1)), the delay margin $\Delta\bar{\tau}(\omega_a)$ of (4) satisfies

$$\Delta\bar{\tau}(\omega_a) \geq \frac{\tan^{-1}\frac{\tilde{\omega}_c(\omega_a)}{\omega_a}}{\tilde{\omega}_c(\omega_a)} > \bar{h}(\omega_a), \quad \forall\, \omega_a,$$

where

$$\bar{h}(\omega_a) = \frac{3}{\omega_a + 2\sqrt{\omega_a^2 + \tilde{\omega}_c^2(\omega_a)}}.$$

With the above lower bound for $\Delta\bar{\tau}$ given by $\bar{h}(\omega_a)$ and the asymptotic behaviour given by Theorem 3.5 we can state:

Corollary 3.6: *The optimal value of the delay margin of (4) with $C = C_2$ is lower bounded as*

$$\Delta\bar{\tau}(\omega_a^*(K,\zeta)) > \frac{3}{\alpha\sqrt{K} + 2\sqrt{\alpha^2 K + \tilde{\omega}_c^2(\alpha\sqrt{K})}},$$

where α is the solution to (13) and $\tilde{\omega}_c$ is defined as in (12).

3.3 Analysis of the lead-lag filter C_3

A lead compensator increases the system crossover frequency and makes the plant very sensitive to high-frequency noise. To mitigate the high-frequency noise amplification while making the filter proper, we can replace $C_2(s)$ by a lead-lag filter as

$$C_3(s) = \frac{\frac{s}{\omega_a} + 1}{\frac{s}{\omega_b} + 1}, \quad \omega_a,\, \omega_b > 0.$$

The frequency ω_b should be selected to prevent delay margin deterioration. The goal of this section is to obtain the achievable delay margin with a lead-lag structure. Namely, to study the effect of parameters ω_a and ω_b on the delay margin of system (4) controlled by C_3.

Proposition 3.7: *Let G be given by (4), with P given by (5), where $K > 0$ and $\zeta > 0$.*

(i) *The delay margin of G with $C = C_3$ is infinite if and only if*

$$\begin{cases} K \leq 1, \\ \omega_b^2 \geq 2 - 4\zeta^2, \\ \dfrac{1}{\omega_b^2} - \dfrac{K^2}{\omega_a^2} \geq 2 - 4\zeta^2, \end{cases} \quad \text{or} \quad \begin{cases} K \leq 1, \\ -4p^3 - 27q^2 < 0, \end{cases} \tag{14}$$

where

$$p = 1 - \frac{(2-4\zeta^2)^2}{3} - \left(\frac{2-4\zeta^2}{3} + \frac{K^2}{\omega_a^2}\right)\omega_b^2 - \frac{\omega_b^4}{3}$$

and

$$q = \frac{2-4\zeta^2}{3} - \frac{2(2-4\zeta^2)^3}{27} + \left(\frac{2}{3} - K^2 - \frac{(2-4\zeta^2)^2}{9} - \frac{(2-4\zeta^2)K^2}{3\omega_a^2}\right)\omega_b^2 + \left(\frac{2-4\zeta^2}{9} + \frac{K^2}{3\omega_a^2}\right)\omega_b^4 + \frac{2\omega_b^6}{27};$$

(ii) *If (14) does not hold, and $\omega_b \geq \omega_a$, then, the delay margin $\Delta\bar{\tau}(\omega_a, \omega_b)$ is given by*

$$\Delta\bar{\tau}(\omega_a,\omega_b) = \begin{cases} \dfrac{\tan^{-1}\frac{(\omega_b-\omega_a)\omega_c}{\omega_b\omega_a+\omega_c^2} + \tan^{-1}\frac{2\zeta\omega_c}{\omega_c^2-1}}{\omega_c}, & \text{if } \omega_c > 1, \\ \dfrac{\pi}{2} + \tan^{-1}\dfrac{\omega_b-\omega_a}{\omega_b\omega_a+1}, & \text{if } \omega_c = 1, \\ \dfrac{\tan^{-1}\frac{(\omega_b-\omega_a)\omega_c}{\omega_b\omega_a+\omega_c^2} - \tan^{-1}\frac{2\zeta\omega_c}{1-\omega_c^2} + \pi}{\omega_c}, & \text{if } \omega_c < 1, \end{cases}$$

where ω_c is a function of ω_a and ω_b, given by the maximum real positive root of the polynomial equation

$$\frac{\omega_c^6}{\omega_b^2} + \left(1 - \frac{2-4\zeta^2}{\omega_b^2}\right)\omega_c^4 - \left(\frac{K^2}{\omega_a^2} + 2 - 4\zeta^2 - \frac{1}{\omega_b^2}\right)\omega_c^2 + 1 - K^2 = 0.$$

Proof: Similar to the proof of Proposition 3.3. ■

Proposition 3.8: *Given the system in (5) without delay, the system is unstable with filter C_3 if and only if*

$$\frac{\omega_b}{\omega_a} < \frac{\frac{\omega_b + K\omega_b}{\omega_b + 2\zeta} - 1 - 2\zeta\omega_b}{K}.$$

Proof: The claim is an immediate consequence of the Routh stability criterion in dimension 3, as detailed in Zabczyk (2002, Theorem 2.4). ■

In Figure 7, for the pair of parameters $K = 35$ and $\zeta = 0.17$, we depict the delay margin contours as a function of the parameters ω_a and ω_b of the filter C_3. To simplify the illustration of these curves we use $\omega_a = \rho\omega_b$, with positive values of ρ. The dashed black curve gives the value of ρ that maximises the delay margin, as a function of ω_b, defined by

$$\rho^*(\omega_b) = \arg\max_{\rho} \{\Delta\bar{\tau}(\rho\omega_b, \omega_b)\},$$

which is obtained with a line search; at every point ω_b, we obtain the value of ρ that maximises the delay margin.

As indicated by Theorem 3.5, for large values of K, the asymptotic behaviour of the optimal values of parameter ω_a, using C_2, is $\omega_a^*(K,\zeta) \approx \alpha\sqrt{K}$. In Figure 7, the solid line corresponds to $\omega_a = \alpha\sqrt{K}$, thus to the points verifying $\rho = \alpha\sqrt{K}/\omega_b$. For large values of ω_b, filter C_3 is equivalent to filter C_2. Hence, following Theorem 3.5, with a large value of K (which is the case in the example since $K = 35$), we should retrieve the maximal values of the delay margins achievable with C_2 taking $\omega_a^*(K,\zeta) = \alpha\sqrt{K}$, for large values of ω_b. For large values of ω_b, we also observe this asymptotic behaviour when the optimal delay margin curve approaches the predicted curve for C_2.

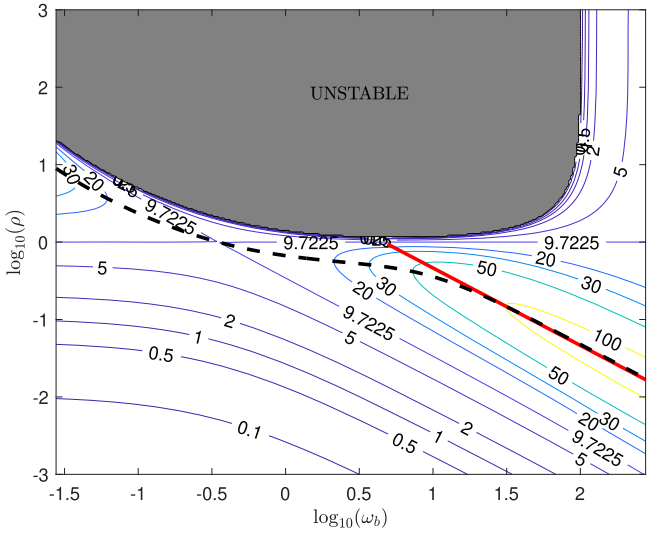

Figure 7. Delay margin contours, in (ms), for $K = 35$ and $\zeta = 0.17$.

3.4 Dynamic compensation-based filters C_4 and C_5

Finally, we consider the filter

$$C_4(s) = \frac{s^2 + 2\zeta_f s + 1}{\left(\frac{s}{\omega_p} + 1\right)\left(\frac{s}{\omega_q} + 1\right)}, \tag{15}$$

already studied in Zaremba et al. (1997). Imposing $\zeta_f = \zeta$ in this filter introduces a compensation of the stable dynamics of $P(s)$ and transforms it into

$$\begin{aligned} L(s) &= P(s)C_4(s) \\ &= \frac{K}{s^2 + 2\zeta s + 1} \frac{s^2 + 2\zeta s + 1}{\left(\frac{s}{\omega_p} + 1\right)\left(\frac{s}{\omega_q} + 1\right)} \\ &= \frac{K}{\frac{s^2}{\omega_p\omega_q} + 2\left(\frac{1}{2\omega_p} + \frac{1}{2\omega_q}\right)s + 1}. \end{aligned}$$

From this expression, the analysis of filter C_4 can be derived from Proposition 3.1, since it is the same transfer function for the feedback loop of the system, with

$$\zeta = \left(\frac{1}{2}\sqrt{\frac{\omega_q}{\omega_p}} + \frac{1}{2}\sqrt{\frac{\omega_p}{\omega_q}}\right) \quad \text{and} \quad \omega_0 = \sqrt{\omega_p\omega_q}. \tag{16}$$

Moreover, to further increase the delay margin, the filter (15) could also be combined with a lead compensator (9), thus resulting in the filter

$$C_5(s) = \frac{\left(s^2 + 2\zeta_f s + 1\right)\left(\frac{s}{\omega_a} + 1\right)}{\left(\frac{s}{\omega_p} + 1\right)\left(\frac{s}{\omega_q} + 1\right)}.$$

In this case, the analysis is equivalent to that of Section 3.2 since

$$\begin{aligned} L(s) &= P(s)C_5(s) \\ &= \frac{K\left(\frac{s}{\omega_a} + 1\right)}{\frac{s^2}{\omega_p\omega_q} + 2\left(\frac{1}{2\omega_p} + \frac{1}{2\omega_q}\right)s + 1}. \end{aligned}$$

Unlike the lead and lead-lag filters, where the maximum achievable delay margin with fixed values of K and ζ is limited when (6) does not hold, the filters C_4 and C_5 can arbitrarily increase the delay margin of a stable system by compensating system poles and introducing well-damped ones. However, even if the filter zeros exactly compensate the system poles, a well-damped system dynamics can decrease the performance of the system in terms of the steering feel and the road feel.

3.5 Stability of the coupled system and disturbance rejection

In contrast with the previous sections, where the coupling between the two subsystems was not taken into account, here we analyse the stability of the electric power steering system considering the coupling between the steering wheel and the pinion subsystems. Moreover, the sensitivity of the proposed controller with respect to input disturbances is also considered.

Usually, in an electric power steering system, the driver torque is estimated using the torque sensor. In fact, the driver torque can be written as $T_d = T_s + \delta_d = k_s(\theta_w - \theta_p) + \delta_d$, where δ_d is the error between the driver torque input T_d and the measured signal T_s. Introducing this last expression in (1), the electric power steering system can be represented in the Linear Fractional Transformation (LFT) form as shown in Figure 8, where v is defined as

$$v(s) = \frac{(\mathrm{e}^{-\tau s} - 1)k_s(\theta_w(s) - \theta_p(s))}{\tau s}$$

and the system Σ is defined by

$$k_s(\theta_w(s) - \theta_p(s)) = G_v(s)v(s) + G_d(s)\delta_d(s) + G_r(s)T_r(s), \tag{17}$$

where

$$G_v(s) = -\frac{\tau s K k_s C(s)}{J_p s^2 + \sigma_p s + k_s + K k_s C(s)},$$

$$G_d(s) = \frac{(J_p s^2 + \sigma_p s)k_s}{(J_p s^2 + \sigma_p s + k_s + K k_s C(s))(J_w s^2 + \sigma_w s)},$$

and

$$G_r(s) = \frac{k_s}{J_p s^2 + \sigma_p s + k_s + K k_s C(s)}.$$

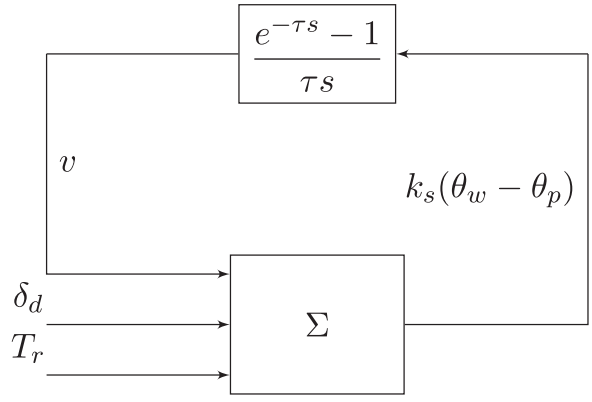

Figure 8. LFT representation of the EPS system.

Note that

$$\left|\frac{e^{-\tau s}-1}{\tau s}\right| \leq 1.$$

From the above feedback loop, we can analyse the stability with respect to the delay by applying the small gain theorem (Lu et al., 1991), therefore yielding the stability of the feedback loop if

$$|G_v(s)| \leq 1.$$

Moreover, to guarantee disturbance rejection with respect to road torque noise, the filter must ensure a small magnitude for the transfer function G_r in the high-frequency range. At steady state, the magnitude of the transfer function G_r is equal to $1/(1+K)$, for all structures of filters C. This transfer function must also have a sufficient bandwidth to provide the driver a feedback torque of the forces acting on the wheels (X. Ma et al., 2018). In addition, to guarantee disturbance rejection with respect to driver torque estimation error, the filter must ensure a small magnitude for the product $G_d(s)\delta_d(s)$ over the whole frequency range. At steady state, from (1), we have $T_d(0) = k_s(\theta_w(0) - \theta_p(0))$, hence $\delta_d(0) = 0$ and therefore $|G_d(0)\delta_d(0)| = 0$. In the high-frequency range, the magnitude of the transfer function G_d must be small. In Section 4.6, these criteria on the transfer functions G_d and G_r are checked over the whole frequency-domain range to assess disturbance rejection for the considered set of system and control parameters.

Remark 3.3: *In standard vehicle designs, a self-alignment torque is produced at the wheels, aiming to return them to the centre position. This torque results from the reaction forces generated by the contact between the tires and the road. Even if this torque stabilises the steering system and increases its robustness, in the stability analysis of the coupled system, we considered the worst-case scenario, in which $T_r = 0$ Nm – see, e.g. Diab et al. (2022). Therefore the above analysis is pessimistic since it neglects an additional stabilising torque.*

4. Simulations

To illustrate the theoretical results of Section 3, we simulate the EPS system using the parameter values detailed in Table 1. These values are taken from D. Lee, Kim, et al. (2018), in which a standard column-type EPS system is considered (corresponding to a Hyundai Motors i30 vehicle). In Sections 4.1 and 4.2, we illustrate numerically the results of Theorems 3.4 and 3.5 obtained for the lead filter C_2. These simulations give an insight of the delay margin achievable using C_2. Then, in Section 4.3, we compare the delay margins obtained using the filter structures described in Table 2. Afterward, in Section 4.4, we compare these filters considering the steering and road feel performances of the EPS system. In Section 4.5, we test the robustness of our filter face to a time-varying delay. Finally, in Section 4.7, we provide a comparison with a recent controller in the literature (D. Lee, Kim, et al., 2018), where the controller design is based on the solution to an optimisation problem without taking into account the delay margin of the system. To present realistic values for parameters ω_a, ω_b, ω_p, and ω_q, we use their actual (non-normalised) values (see Remark 2.1).

4.1 Maximum achievable delay margin with a lead filter

In Figure 9(a), we consider the plant (5) with the filter C_2, in which we allow the assist gain K to vary in the interval $[1, 100]$, fixing $\zeta = 0.17$, see Table 1. For each value of K, we compare the value of $\omega_a^*(K,\zeta)$ with its upper bound and its asymptote $\alpha\sqrt{K}$ using the results of Theorems 3.4 and 3.5, respectively. For a large value of the assist gain K, Figure 9(a) illustrates the asymptotic behaviour outlined in Theorem 3.5. Figure 9(b) shows the delay margin obtained using the three values presented in Figure 9(a), namely, the optimal value $\omega_a^*(K,\zeta)$, its upper bound, and its asymptotic value. Note that the delay margin curve computed with $\omega_a = \omega_a^*$ is an upper bound for the other two curves and converges asymptotically to the red curve, for large values of K. Since our filters were designed for a normalised frequency, the delay margins for the actual system are recovered by dividing the result by ω_0 (which is dimensionless). Figure 9(b) shows that, for $K > 1$, the maximum achievable delay margin with filter C_2 is limited.

4.2 Analytical approximation of the delay margin for the lead filter

In the remainder of this section, we fix $K = 35$ and $\zeta = 0.17$, as in D. Lee, Kim, et al. (2018). Following Proposition 3.3, we compute the maximum achievable delay margin for $K = 35$, which is equal to $\Delta\bar{\tau}(\omega_a^*(35, 0.17)) = 3.58$ ms. In Theorem 3.4, we showed that for a given value of the assist gain K and a given value of the damping coefficient ζ of the EPS system, the value of the lead filter parameter that maximises the delay margin of the EPS system is upper-bounded by $\bar{\omega}_a^*$. Then, to estimate the delay margin achievable with a lead filter, we approximate the parameter of the lead filter by the explicit value of its upper bound $\omega_a = \bar{\omega}_a^*$, given in Theorem 3.4. For $\omega_a = \bar{\omega}_a^* = 40.39$ Hz, the delay margin is 3.27 ms compared to the maximum achievable delay margin 3.58 ms obtained at $\omega_a = \omega_a^* = 27.48$ Hz. The value ω_a^* giving the maximum delay margin is obtained by solving the implicit equation corresponding to (A9) in the Appendix, with its left-hand side set to zero. Figure 10 shows the achievable delay margin of the EPS system with a lead filter in function of the filter parameter. The figure illustrates that Theorem 3.4 gives a close approximation of the achievable delay margin.

4.3 Comparison between the delay margins of the different filter structures

Recall that $C_1(s) = 1$. For the lead filter C_2, we set the parameter of this filter at the value $\omega_a = \omega_a^*$ that achieves the maximum delay margin. For the lead-lag filter C_3, we chose $\omega_a = \omega_a^*$ in the same way as for the lead filter and we add a lag that corresponds to a more realistic implementation of this filter, fixing the parameter ω_b to the highest possible value allowed by the sensor noise level. Following D. Lee, Kim, et al. (2018), we set ω_b to 159.15 Hz.

EPS systems must have sufficient bandwidth to respond seamlessly to the fastest driver inputs while maintaining road feel through the mechanical steering mechanism (Marouf et al., 2012). In D. Lee, Kim, et al. (2018), a nonlinear optimisation problem is solved to maximise the phase margin and the

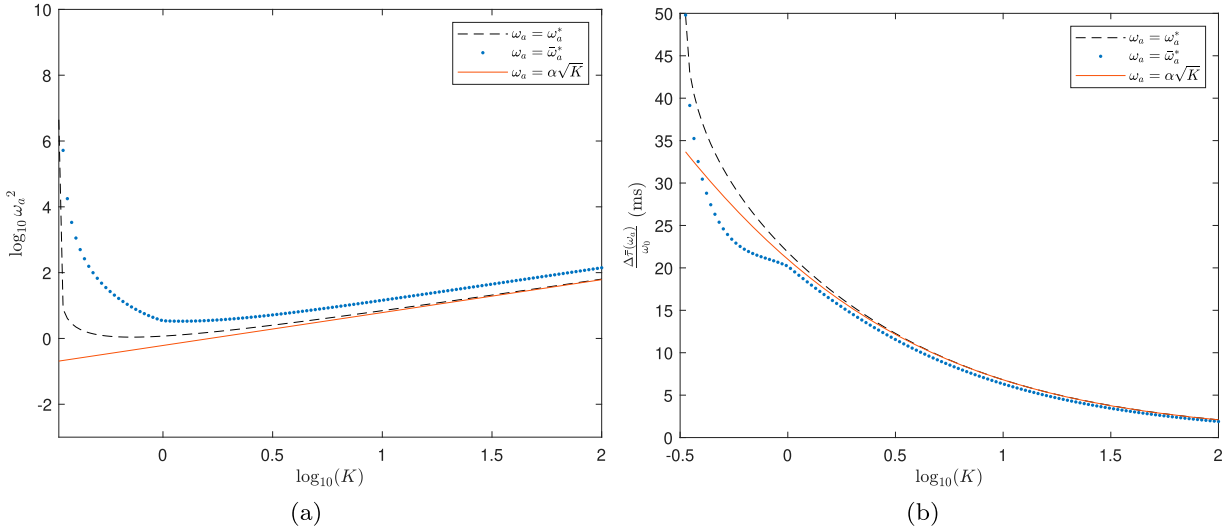

Figure 9. (a) Upper bound and asymptotic value of ω_a^* as a function of K. (b) Comparison between the different delay margin bounds (for filter C_2) with the choice of ω_a resulting from Theorems 3.4 and 3.5.

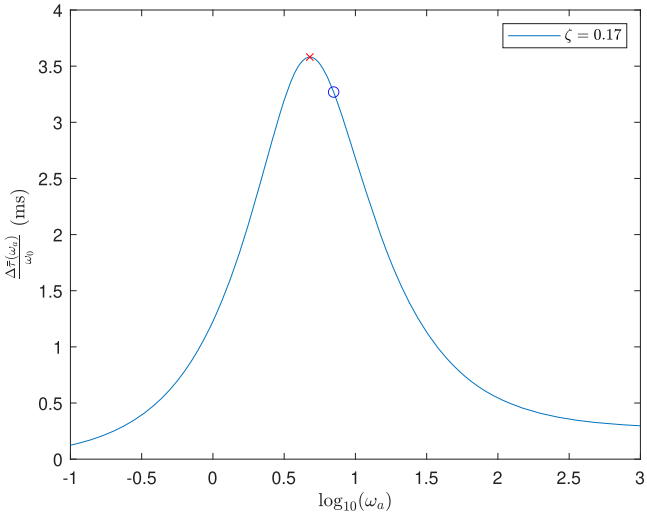

Figure 10. Delay margin as a function of ω_a, for $K = 35$ and $\zeta = 0.17$: The red cross corresponds to the optimal delay margin for the optimal value ω_a^*, while the blue circle provides the upper bound $\bar{\omega}_a^*$ and the corresponding delay margin, given by Theorem 3.4.

gain margin of the controlled system. In Zaremba et al. (1998), the bandwidth is considered in the optimal synthesis procedure of the controller to balance between useful information transmitted from the road to the driver and the unwanted disturbance and noise. In our approach, we select C_4 to satisfy the following items:

(i) Compensate the dynamics of the EPS system, that is $\zeta_f = \zeta$;
(ii) Preserve the bandwidth for the initial EPS system, that is $\omega_p\omega_q = \omega_0^2$;
(iii) Set the delay margin to 5.00 ms.

Finally, the parameters of the filter C_5 are selected to satisfy the following items:

(i) Compensate the dynamics of the EPS system, that is $\zeta_f = \zeta$;
(ii) Preserve the same bandwidth for the initial EPS system, that is $\omega_p\omega_q = \omega_0^2$;
(iii) Set the delay margin to 5.00 ms with $\omega_a = \omega_a^*$.

Table 3 summarises the values of the filter parameters and the corresponding delay margin for the system parameters of Table 1, and three values for parameter σ_p: $\sigma_p = 1.35$ Nm.s/rad, $\sigma_p = 12.18$ Nm.s/rad, and $\sigma_p = 16.79$ Nm.s/rad. A higher delay margin can be achieved with the filters C_4 and C_5 following the discussion in Section 3.4. However, this degrades the performance of the system, evaluated in terms of steering and road feel. The differences in the performance between two filters giving the same delay margin are discussed below.

4.4 Comparison between different filter structures in terms of steering feel and road feel

We now set the value of the delay in the feedback loop to $\tau = 4$ ms. We will study three different cases corresponding to the three different values of parameter σ_p detailed in Table 3.

To illustrate the behaviour of the obtained filters, we consider two criteria. The first criterion (the 'road feel'), is assessed by the driver torque T_d that would be required to keep the steering wheel at $\theta_w = 0$ deg. Namely, the torque T_d^* satisfying $T_d^* = -k_s\theta_p$. In this situation, the input to the steering wheel dynamics (in the bottom of Figure 3) is equal to zero. This torque from the driver then eliminates the effect of the road reaction torque on the steering wheel. From the system equations, we obtain the following transfer function

$$\frac{T_d^*(s)}{T_r(s)} = \frac{k_s}{J_p s^2 + \sigma_p s + k_s + Kk_s C(s)\,\mathrm{e}^{-\tau s}}. \tag{18}$$

An illustrative frequency response of the transfer function (18) is represented in Figure 12(b). Steering systems must have sufficient bandwidth to respond seamlessly to the driver fastest inputs while at the same time preserving the feel of the road through the mechanical steering mechanism (Zaremba et al., 1997). Moreover, the resonance peak must be limited to

Table 3. Delay margin of the pinion subsystem obtained with the different filter structures analysed in this paper.

Filter	$C_1(s)$	$C_2(s)$	$C_3(s)$	$C_4(s)$	$C_5(s)$
Structure	1	$\frac{s}{\omega_a}+1$	$\frac{\frac{s}{\omega_a}+1}{\frac{s}{\omega_b}+1}$	$\frac{\frac{s^2}{\omega_0^2}+\frac{2\zeta}{\omega_0}s+1}{\left(\frac{s}{\omega_p}+1\right)\left(\frac{s}{\omega_q}+1\right)}$	$\frac{\left(\frac{s^2}{\omega_0^2}+\frac{2\zeta}{\omega_0}s+1\right)\left(\frac{s}{\omega_a}+1\right)}{\left(\frac{s}{\omega_p}+1\right)\left(\frac{s}{\omega_q}+1\right)}$
Filter parameters (Hz)		$\omega_a = 27.48$	$\omega_a = 27.48$	$\omega_p = 1.07$	$\omega_p = 2.13$
$\sigma_p = 1.35$ Nm.s/rad			$\omega_b = 159.15$	$\omega_q = 30.75$	$\omega_q = 15.50$
					$\omega_a = 35.67$
Delay margin (ms)	0.27	3.58	2.69	5.00	5.00
Filter parameters (Hz)		$\omega_a = 35.67$	$\omega_a = 35.67$	$\omega_p = 1.07$	$\omega_p = 2.13$
$\sigma_p = 12.18$ Nm.s/rad			$\omega_b = 159.15$	$\omega_q = 30.75$	$\omega_q = 15.50$
					$\omega_a = 35.67$
Delay margin (ms)	2.54	5.00	4.13	5.00	5.00
Filter parameters (Hz)		$\omega_a = 39.15$	$\omega_a = 39.15$	$\omega_p = 1.07$	$\omega_p = 2.13$
$\sigma_p = 16.79$ Nm.s/rad			$\omega_b = 159.15$	$\omega_q = 30.75$	$\omega_q = 15.50$
					$\omega_a = 35.67$
Delay margin (ms)	3.64	5.87	5.00	5.00	5.00

Notes: The default system parameters are reported in Table 1. Additional settings of pinion damping σ_p were considered to increase the value of the delay margin.

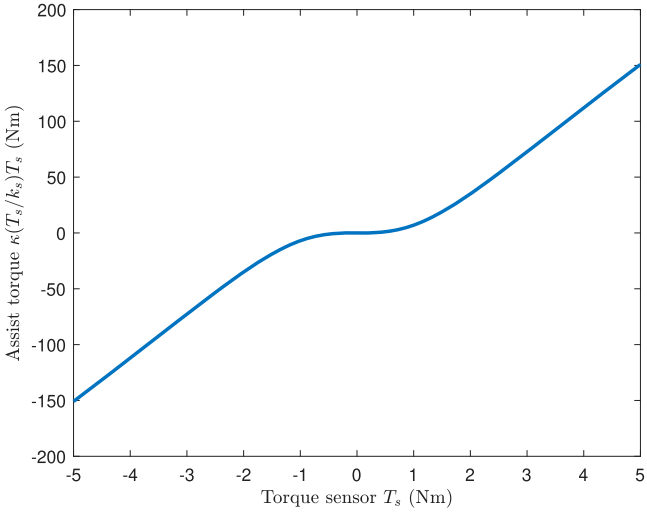

Figure 11. Torque map of the EPS.

prevent vibrations in the steering wheel that can worsen the driver feeling of the road forces. For the second criterion (the 'steering feel'), the EPS system is simulated under a steering input signal given by a sinusoid of amplitude 30 deg and of frequency 0.2 Hz, applied during a single period. Differently from the 'road feel' assessment test, a nonlinear torque map, the function κ in (2), has been included to provide a more realistic representation of the steering feel (Y. Li et al., 2018, Figure 8). The considered torque map is represented in Figure 11. For the obtained trajectory, we plot the driver steering torque T_d as a function of the steering wheel angle θ_w. The steering feel is quantified from the 'hysteresis' curves of driver steering torque versus steering wheel angle given by sinusoidal input. The amplitude of the steering wheel angle for the zero steering wheel torque is used to quantify the hysteresis. The higher the hysteresis is, the worse the steering feel is for the driver. An illustration of the hysteresis curve is provided in Figure 12(d).

First case ($\sigma_p = 1.35$ Nm.s/rad). In this case, for filters C_1, C_2, and C_3, the feedback loop is unstable since the Nyquist plots of C_1, C_2, and C_3 encircle the critical point (Figure 12(a)). Indeed, the delay margins in Table 3 are smaller than 4 ms for C_1, C_2, and C_3, when $\sigma_p = 1.35$ Nm.s/rad. In Figure 12(b), for C_4 and C_5, the closed-loop transfer function of the road reaction torque to the driver torque T_d^* exhibits two resonant frequencies. These resonances may produce vibrations that are transmitted to the steering wheel and degrade the road feel. Figure 12(c) shows the time response of the torque required by the driver to lock the steering wheel in the centre position for an input road torque signal given by a sequence of constant values. The figure shows that the response with filter C_5 presents a slightly faster response and smaller overshoot. For the same delay margin, the filter C_4 has poorer performance than C_5. As shown in Figure 12(d), the filter C_4 presents a larger hysteresis, associated with an increased damping of the steering system. This slightly reduces the steering feel. Moreover, the filters C_4 and C_5 allow for arbitrarily high delay margins, a property that cannot be obtained using C_2 (see Proposition 3.3). However, the filters C_2 and C_5 are not realistic. For this reason, we must consider the second and third cases described below, where we increase the value of the pinion damping to make filter C_3 stable in the presence of the prescribed delay.

Second case ($\sigma_p = 12.18$ Nm.s/rad). In this case, except for C_1, all filters considered in Table 2 ensure a stable feedback loop – see Table 3. With filter C_2, the feedback loop can achieve a delay margin of 5.00 ms. But, since this is an ideal filter, the value of the pinion damping has to be further increased to achieve a delay margin of 5.00 ms with filter C_3, which can be implemented physically.

Third case ($\sigma_p = 16.79$ Nm.s/rad). As in the previous case, except for C_1, all filters considered in Table 2 ensure a stable feedback loop with the delay $\tau = 4$ ms, as it can be observed in Figure 13(a). In Figure 13(b), we show that filter C_3 can improve the bandwidth of the closed-loop transfer function of the road reaction torque to the driver torque T_d^* and reduce the resonant frequency. Figure 13(c) shows that the response with the filter C_3 presents a slightly smaller time constant but also reduced overshoot. The filter C_4 has a poorer performance than C_3 for the same delay margin. As shown in Figure 13(d), filter C_4 presents a larger hysteresis, associated with an increased damping of the steering system. This hysteresis generates an additional force that the driver must provide during manoeuvres.

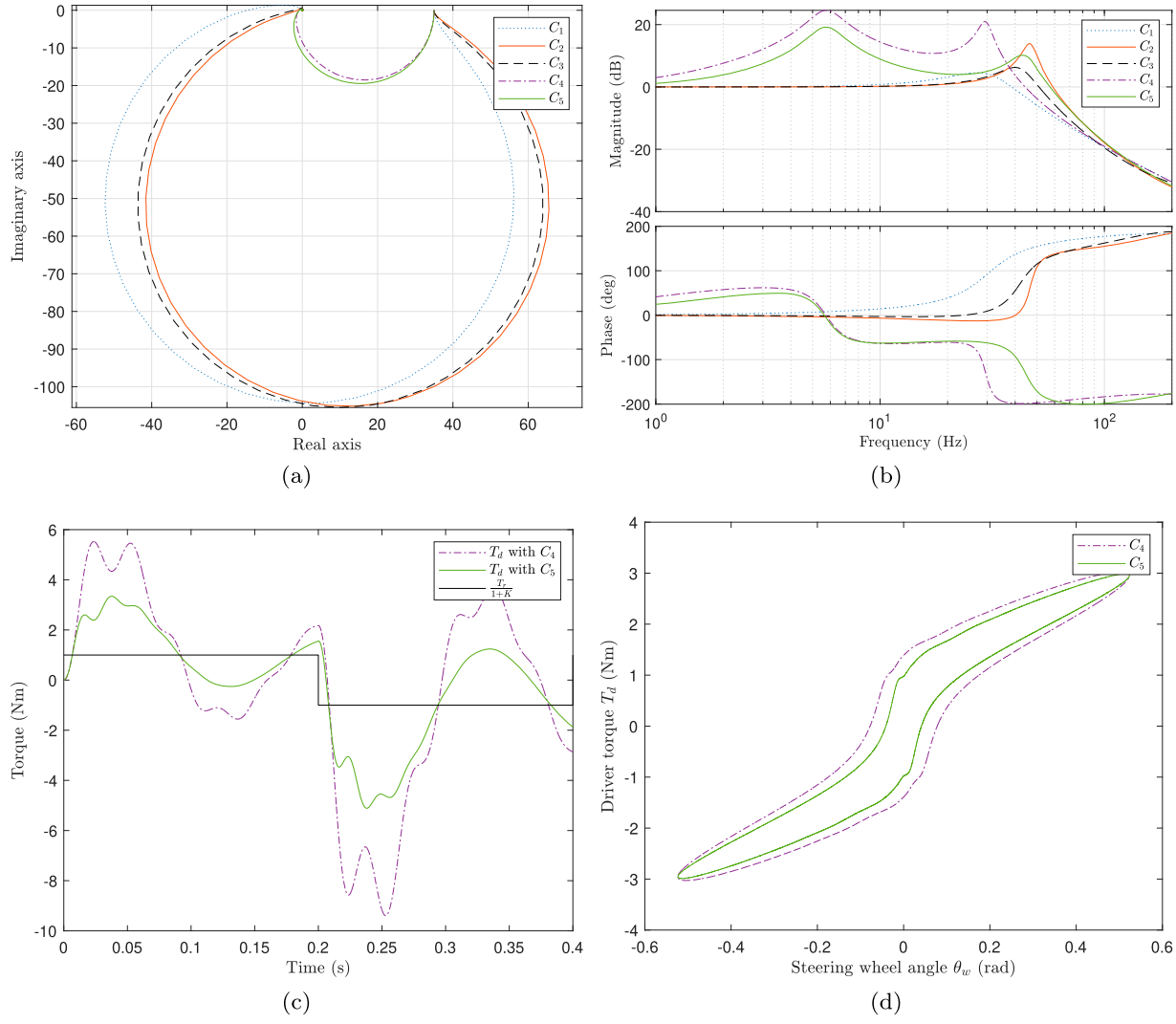

Figure 12. *First case* ($\sigma_p = 1.35$ Nm.s/rad). Top: (a) Nyquist plot of $L(s) = P(s)C(s)\,e^{-\tau s}$. (b) Frequency responses of the road reaction torque to the driver torque. Bottom: Driver comfort assessment tests. (c) Driver torque for a road torque input given by a square signal. (d) Hysteresis curve to assess the steering feel.

Table 4. Summary of the comparison between the five considered filter structures.

Filter	Advantages	Drawbacks
C_1	Standard filter in the case without delay	Poor delay margin
C_2	Increases the delay margin Preserves steering system performance	Limited delay margin Non-causal filter
C_3	Increases the delay margin Preserves steering system performance	Limited delay margin
C_4	Arbitrarily high delay margin	Degrades the steering system performance
C_5	Arbitrarily high delay margin	Degrades the steering system performance Non-causal filter

Table 4 summarises the advantages and drawbacks of each filter structure in terms of the stability margins as well as the performance of the steering system.

4.5 Time-varying delay case

In this section, we consider filter C_3 with $\sigma_p = 16.79$ Nm.s/rad, which is the one that provided the best performance in Section 4.4. For this filter, we simulate a time-varying delayed signal to test its robustness to a time-varying delay. The tests were carried out considering time-varying delays within the delay range for which the stability is guaranteed for fixed delays. We considered a time-varying delay (in ms) of the form

$$\tau(t) = \tau_0 + \epsilon \sin(\omega t),$$

where $\tau_0 = 4$ ms. Simulations are illustrated in Figures 14(a,b), where the considered values of parameters ω and ϵ are provided in the legend of each plot. It is shown that the variations of the delay around a constant average value, as in the above expression, do not have a significant effect on the performance of the filter.

4.6 Controller sensitivity with respect to rejection of disturbances

In this section, we also consider filter C_3 with $\sigma_p = 16.79$ Nm.s/rad. For this filter, we plot in Figure 15 the Bode diagrams of the transfer functions G_d and $(1 + K)G_r$. We considered a constant delay $\tau = 4$ ms. It is shown that the magnitudes of the

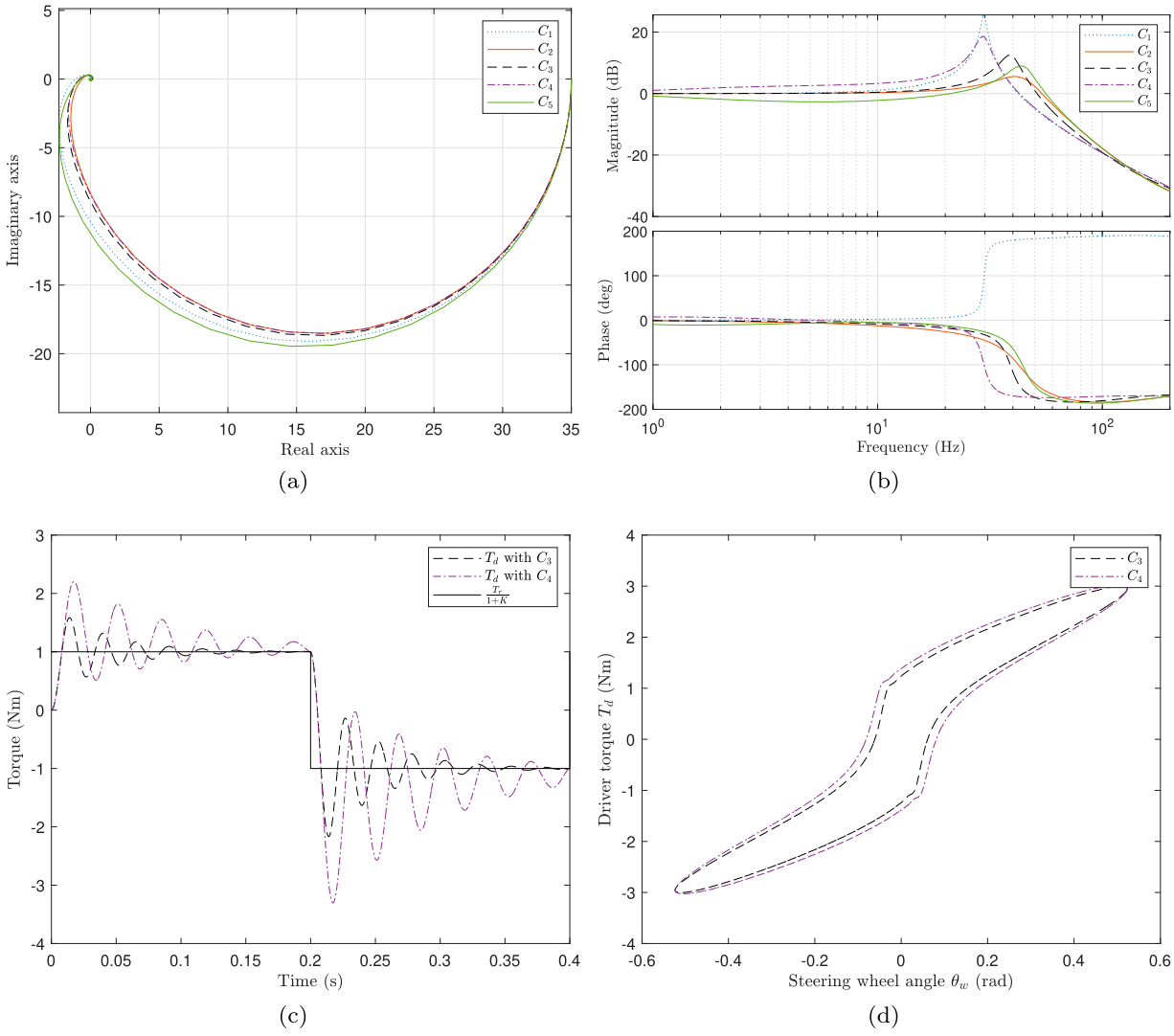

Figure 13. *Third case* ($\sigma_p = 16.79$ Nm.s/rad). Top: (a) Nyquist plot of $L(s) = P(s)C(s)\,e^{-\tau s}$. (b) Frequency responses of the road reaction torque to the driver torque. Bottom: Driver comfort assessment tests. (c) Driver torque for a road torque input given by a square signal. (d) Hysteresis curve to assess the steering feel.

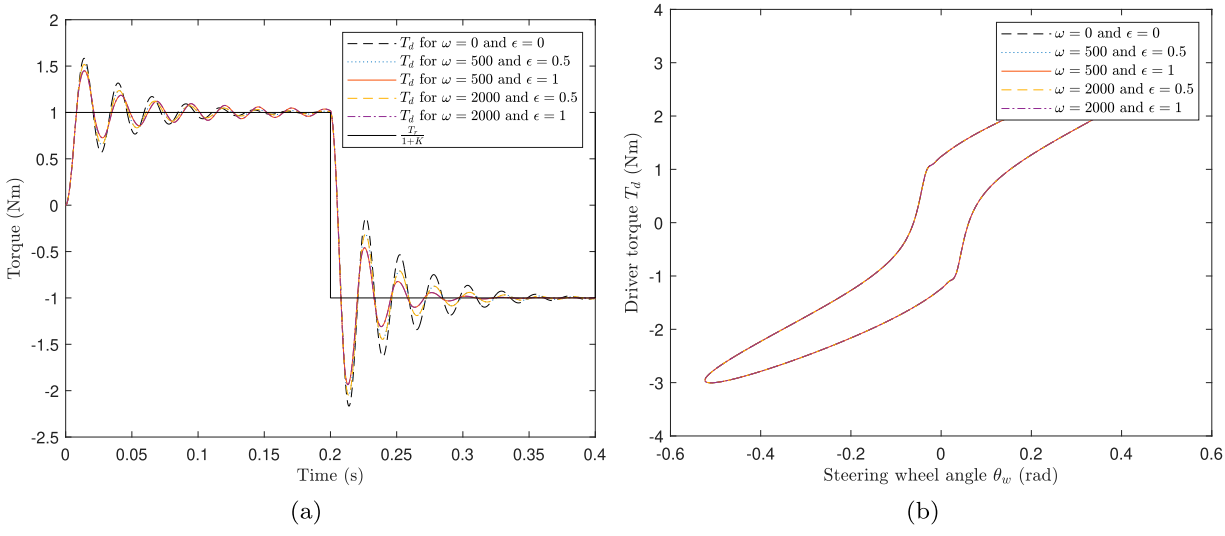

Figure 14. Driver comfort assessment tests for $\sigma_p = 16.79$ Nm.s/rad, with a time-varying delay. (a) Driver torque for a road torque input given by a square signal. (b) Hysteresis curve to assess the steering feel.

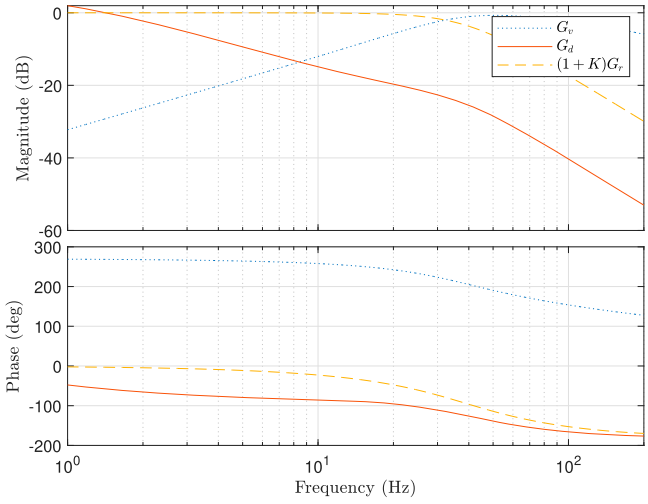

Figure 15. Frequency responses of the transfer function G_d, G_r, and G_v for $\sigma_p = 16.79$ Nm.s/rad, with a constant delay $\tau = 4$ ms.

transfer functions G_d and G_r are small in the high-frequency range. Moreover, the transfer function G_r has a sufficiently large bandwidth that provides the driver feedback on the force acting on the wheels.

4.7 Comparison with existing results

In this section, a comparison with a recent state-of-the-art controller is carried out. For the parameters values given in Table 1 with $\sigma_p = 1.35$ Nm.s/rad, the selected optimal controller proposed in D. Lee, Kim, et al. (2018) is a cascade of three lead-lag filters, given by

$$C_6(s) = \frac{\left(\frac{s}{55.3}+1\right)\left(\frac{s}{32.7}+1\right)\left(\frac{s}{80.2}+1\right)}{\left(\frac{s}{1000}+1\right)\left(\frac{s}{6}+1\right)\left(\frac{s}{713}+1\right)}.$$

The design of the above control does not take into account delays in the loop. We measured the delay margin of the above controller to be 1.8 ms, which is significantly smaller in comparison to the delay margin of 2.69 ms of C_3. Moreover, for a delay of 1.5 ms, we apply the road feel and steering feel tests and, for both tests, a worse performance is obtained for C_6 as illustrated in Figure 16.

5. Conclusions

Motivated by its applications to the analysis of EPS systems stability, we studied a feedback loop consisting of a second-order system in feedback with a control filter and delays. Since the analytic expression of exact delay margins is difficult to obtain, explicit formulas to lower bound them were proposed. For different filter configurations, we showed that improved delay margins could be obtained by reducing the assist gain or by increasing the damping of the system. However, in addition to the robustness with respect to delays, the simulation results indicate that an increased damping can have a negative impact on the subjective steering feel and road feel performances. Future work will propose a trade-off between performance measures (in terms of steering feel and road feel) and delay margins.

Disclosure statement

No potential conflict of interest was reported by the author(s).

ORCID

Ali Diab http://orcid.org/0000-0003-0992-9417

References

Baek, J., & Kang, C. (2020). Time-delayed control for automated steering wheel tracking of electric power steering systems. *IEEE Access*, *8*, 95457–95464. https://doi.org/10.1109/Access.6287639

Boros, G., & Moll, V. H. (2005). Sums of arctangents and some formulas of Ramanujan. *Scientia*, *11*(540623), 13–24.

Chen, X., Yang, T., Chen, X., & Zhou, K. (2008). A generic model-based advanced control of electric power-assisted steering systems. *IEEE Transactions on Control Systems Technology*, *16*(6), 1289–1300. https://doi.org/10.1109/TCST.2008.921805

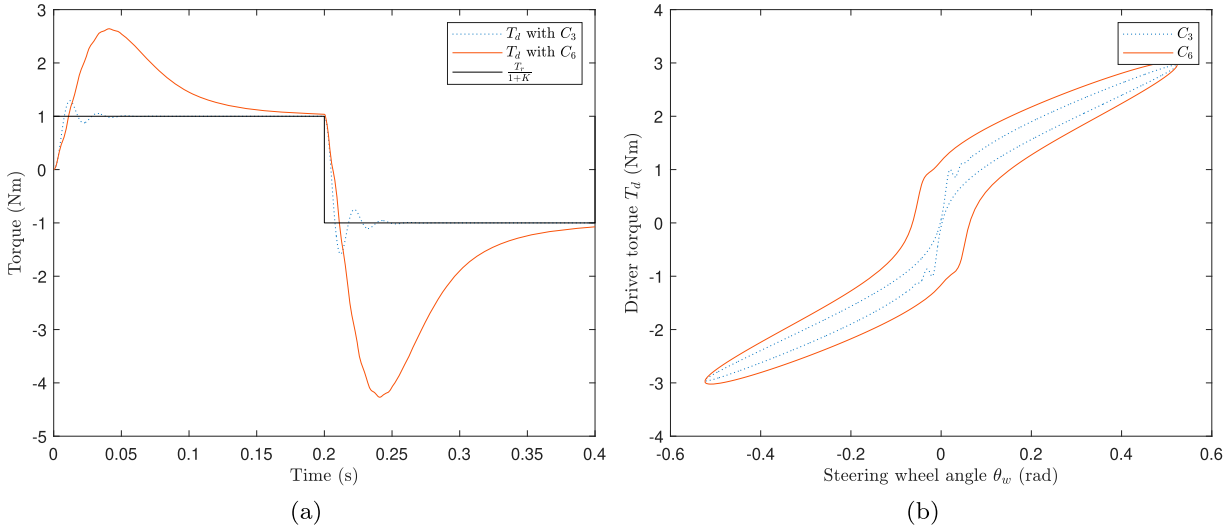

(a) (b)

Figure 16. Driver comfort assessment tests for $\sigma_p = 1.35$ Nm.s/rad, with a constant delay $\tau = 1.5$ ms. (a) Driver torque for a road torque input given by a square signal. (b) Hysteresis curve to assess the steering feel.

Diab, A., Pasillas-Lépine, W., & Valmorbida, G. (2022). A steer-by-wire control architecture robust to high assistance gains and large transmission delays. In *Proceedings of the International Symposium on Advanced Vehicle Control*.

Lee, D., Jang, B., Han, M., & Kim, K.-S. (2021). A new controller design method for an electric power steering system based on a target steering torque feedback controller. *Control Engineering Practice*, *106*, 104658. https://doi.org/10.1016/j.conengprac.2020.104658

Lee, D., Kim, K., & Kim, S. (2018a). Controller design of an electric power steering system. *IEEE Transactions on Control Systems Technology*, *26*(2), 748–755. https://doi.org/10.1109/TCST.2017.2679062

Lee, D., & Spong, M. W. (2006). Passive bilateral teleoperation with constant time delay. *IEEE Transactions on Robotics*, *22*(2), 269–281. https://doi.org/10.1109/TRO.2005.862037

Lee, D., Yi, K., Chang, S., Lee, B., & Jang, B. (2018b). Robust steering-assist torque control of electric-power-assisted-steering systems for target steering wheel torque tracking. *Mechatronics*, *49*, 157–167. https://doi.org/10.1016/j.mechatronics.2017.12.007

Lee, M. H., Seung, K. H., Choi, J. Y., & Yoon, K. S. (2005). Improvement of the steering feel of an electric power steering system by torque map modification. *Journal of Mechanical Science and Technology*, *19*(3), 792–801. https://doi.org/10.1007/BF02916127

Li, X., Zhao, X.-P., & Chen, J. (2009). Controller design for electric power steering system using ts fuzzy model approach. *International Journal of Automation and Computing*, *6*(2), 198–203. https://doi.org/10.1007/s11633-009-0198-0

Li, Y., Shim, T., Wang, D., & Offerle, T. (2018). Study on parameters affecting steering feel of column assist electric power steering. *International Journal of Vehicle Design*, *77*(3), 153–179. https://doi.org/10.1504/IJVD.2018.098941

Lu, W., Zhou, K., & Doyle, J. (1991). Stabilization of lft systems. In *Proceedings of the Conference on Decision and Control* (Vol. 2, pp. 1239–1244).

Ma, D., Chen, J., Liu, A., Chen, J., & Niculescu, S.-I. (2019). Explicit bounds for guaranteed stabilization by PID control of second-order unstable delay systems. *Automatica*, *100*, 407–411. https://doi.org/10.1016/j.automatica.2018.11.053

Ma, X., Guo, Y., & Chen, L. (2018). Active disturbance rejection control for electric power steering system with assist motor variable mode. *Journal of the Franklin Institute*, *355*(3), 1139–1155. https://doi.org/10.1016/j.jfranklin.2017.12.024

Marouf, A., Djemai, M., Sentouh, C., & Pudlo, P. (2012). A new control strategy of an electric-power-assisted steering system. *IEEE Transactions on Vehicular Technology*, *61*(8), 3574–3589. https://doi.org/10.1109/TVT.2012.2209689

Middleton, R. H., & Miller, D. E. (2007). On the achievable delay margin using LTI control for unstable plants. *IEEE Transactions on Automatic Control*, *52*(7), 1194–1207. https://doi.org/10.1109/TAC.2007.900824

Mortici, C., & Srivastava, H. M. (2014). Estimates for the arctangent function related to Shafer's inequality. *Colloquium Mathematicum*, *136*(2), 263–270. https://doi.org/10.4064/cm136-2-8

Niculescu, S. (2001). *Delay effects on stability: A robust control approach* (Vol. 269). Springer Science & Business Media.

Sugitani, N., Fujuwara, Y., Uchida, K., & Fujita, M. (1997). Electric power steering with H-infinity control designed to obtain road information. In *Proceedings of the American Control Conference* (Vol. 5, pp. 2935–2939).

Yamamoto, K., Sename, O., Koenig, D., & Moulaire, P. (2019). Design and experimentation of an LPV extended state feedback control on electric power steering systems. *Control Engineering Practice*, *90*, 123–132. https://doi.org/10.1016/j.conengprac.2019.06.004

Zabczyk, J. (2002). Classical control theory. In A. Agrachev (Ed.), *Mathematical Control Theory – Part 1* (pp. 1–58). International Atomic Energy Agency (IAEA).

Zaremba, A. T., Liubakka, M. K., & Stuntz, R. M. (1997). Vibration control based on dynamic compensation in an electric power steering system. In *Proceedings of the International Conference on Control of Oscillations and Chaos* (Vol. 3, pp. 453–456).

Zaremba, A. T., Liubakka, M. K., & Stuntz, R. M. (1998). Control and steering feel issues in the design of an electric power steering system. In *Proceedings of the American Control Conference* (Vol. 1, pp. 36–40).

Appendix 1. Technical proofs

The following lemma, see Boros and Moll (2005) and D. Ma et al. (2019), will be used to prove Proposition 3.3 and at several other places of the paper.

Lemma A.1: *Suppose that* $\xi \geq 0$, $\eta \geq 0$. *Then,*

(i) $\tan^{-1}\xi + \tan^{-1}\eta = \begin{cases} \tan^{-1}\dfrac{\xi+\eta}{1-\xi\eta}, & \xi\eta < 1, \\ \dfrac{\pi}{2}, & \xi\eta = 1, \\ \tan^{-1}\dfrac{\xi+\eta}{1-\xi\eta} + \pi, & \xi\eta > 1; \end{cases}$

(ii) $\tan^{-1}\xi - \tan^{-1}\eta = \tan^{-1}\frac{\xi-\eta}{1+\xi\eta}$;

(iii) $\frac{\xi}{1+\xi^2} \leq \tan^{-1}\xi \leq \xi$;

(iv) $0 \leq \tan^{-1}\xi < \frac{\pi}{2}$.

Proof of Proposition 3.3: *Item (i).* Let $\tilde{\omega}_c(\omega_a)$ be the unity-gain crossover frequency of the open-loop transfer function $P(s)C_2(s)$. If it exists, the frequency $\tilde{\omega}_c(\omega_a)$ is necessarily a positive real root of the polynomial equation

$$\tilde{\omega}_c^4(\omega_a) - \left(\frac{K^2}{\omega_a^2} + 2 - 4\zeta^2\right)\tilde{\omega}_c^2(\omega_a) + 1 - K^2 = 0. \tag{A1}$$

Observe that the closed-loop delay margin is infinite if and only if the Nyquist diagram of the open-loop transfer function does not intersect the unity gain circle (at a strictly positive frequency). Hence, to have an infinite delay margin, the above polynomial should not have any strictly positive real root. By Routh's criterion, this is equivalent to condition (10) of the Proposition's first item.

Item (ii). The open-loop transfer function is given by

$$P(s)C_2(s) = \frac{K\left(\frac{s}{\omega_a} + 1\right)}{s^2 + 2\zeta s + 1}. \tag{A2}$$

Denote by p_1 and p_2 the two poles of the system. Since the system is stable, there exist two real numbers $\alpha > 0$ and $\beta \geq 0$ such that $p_1 = -\alpha + j\beta$ and $p_2 = -\alpha - j\beta$. From (A2), we have $\alpha = \zeta$ and $\alpha^2 + \beta^2 = 1$.

Define $s = j\omega$. The phase of the open-loop transfer function is given by

$$\phi(\omega) = \tan^{-1}\frac{\omega}{\omega_a} - \tan^{-1}\frac{\omega+\beta}{\alpha} - \tan^{-1}\frac{\omega-\beta}{\alpha} - \pi.$$

The delay margin is given by

$$\Delta\bar{\tau}(\omega_a) = \frac{\phi(\tilde{\omega}_c(\omega_a)) + \pi}{\tilde{\omega}_c(\omega_a)},$$

where

$$\tilde{\omega}_c(\omega_a) = \sqrt{\frac{\frac{K^2}{\omega_a^2} + 2 - 4\zeta^2 + \sqrt{\left(\frac{K^2}{\omega_a^2} + 2 - 4\zeta^2\right)^2 - 4 + 4K^2}}{2}}$$

is the largest root of Equation (A1). Indeed, $\frac{\mathrm{d}}{\mathrm{d}\omega}\left(\frac{\phi(\omega)+\pi}{\omega}\right)$ is a strictly decreasing function of ω. Using Lemma A.1.(i), we obtain the solutions of the delay margin $\Delta\bar{\tau}(\omega_a)$ stated in the proposition. ■

Proof of Theorem 3.4: At the optimal value ω_a^* we have that $\frac{\mathrm{d}\Delta\bar{\tau}}{\mathrm{d}\omega_a}(\omega_a^*) = 0$. Based on this observation, we have that any interval $I = [\bar{\omega}_a^*, \infty)$ satisfying $\frac{\mathrm{d}\Delta\bar{\tau}(\omega_a)}{\mathrm{d}\omega_a} \leq 0$, $\forall\omega_a \in I$, yields an upper bound $\bar{\omega}_a^*$ for ω_a^*. The goal in the steps detailed below is to obtain small values for $\bar{\omega}_a^*$.

First step. Consider the derivative of $\tilde{\omega}_c(\omega_a)$ in (12) with respect to ω_a,

$$\frac{\mathrm{d}\tilde{\omega}_c(\omega_a)}{\mathrm{d}\omega_a} = -\frac{K^2 X(\omega_a)}{\omega_a^3\tilde{\omega}_c(\omega_a)}, \tag{A3}$$

where

$$X(\omega_a) = \frac{\tilde{\omega}_c^2(\omega_a)}{\sqrt{\left(\frac{K^2}{\omega_a^2} + 2 - 4\zeta^2\right)^2 - 4 + 4K^2}}. \tag{A4}$$

Since we assume that (6) does not hold, following Proposition 3.3.(i), condition (10) does not hold. Therefore $\tilde{\omega}_c(\omega_a)$ is well defined and $\tilde{\omega}_c(\omega_a)$ is

well defined and verifies $\tilde{\omega}_c(\omega_a) > 0, \forall \omega_a > 0$. Moreover,

$$\sqrt{\left(\frac{K^2}{\omega_a^2} + 2 - 4\zeta^2\right)^2 - 4 + 4K^2} > 0, \quad \forall\, \omega_a > 0,$$

therefore $X(\omega_a) > 0$, hence (A3) is negative. It follows that $\tilde{\omega}_c(\omega_a)$ is a strictly decreasing function of ω_a. In addition, from (12) we have

$$\lim_{\omega_a \to +\infty} \tilde{\omega}_c(\omega_a) = \hat{\omega}_c,$$

with $\hat{\omega}_c$ as in (7). Since $\tilde{\omega}_c$ is strictly decreasing on ω_a, the above limit implies

$$\tilde{\omega}_c(\omega_a) > \hat{\omega}_c, \quad \forall\, \omega_a > 0. \tag{A5}$$

In (A4), replacing the expression of $\tilde{\omega}_c(\omega_a)$ given by (12) leads to

$$X(\omega_a) = \frac{\frac{K^2}{\omega_a^2} + 2 - 4\zeta^2 + \sqrt{\left(\frac{K^2}{\omega_a^2} + 2 - 4\zeta^2\right)^2 - 4 + 4K^2}}{2\sqrt{\left(\frac{K^2}{\omega_a^2} + 2 - 4\zeta^2\right)^2 - 4 + 4K^2}}. \tag{A6}$$

We can show that

$$X(\omega_a) \leq \begin{cases} 1, & \text{if } K > 1, \\ c_0, & \text{if } K \leq 1 \quad \text{and} \quad 2\zeta\sqrt{1-\zeta^2} < K. \end{cases} \tag{A7}$$

Indeed, since we assume that (6) does not hold let us consider the two cases below:

- For $K > 1$, (cases I and III)

$$\frac{K^2}{\omega_a^2} + 2 - 4\zeta^2 < \sqrt{\left(\frac{K^2}{\omega_a^2} + 2 - 4\zeta^2\right)^2 - 4 + 4K^2}, \quad \omega_a > 0.$$

  This implies that, from (A6), $X(\omega_a) \leq 1$;
- For $K \leq 1$ and $2\zeta\sqrt{1-\zeta^2} < K$, (cases II and IV)

$$\frac{K^2}{\omega_a^2} + 2 - 4\zeta^2 \geq \sqrt{\left(\frac{K^2}{\omega_a^2} + 2 - 4\zeta^2\right)^2 - 4 + 4K^2}, \quad \omega_a > 0.$$

  In this case, from (A6), we have

$$X(\omega_a) \leq \frac{\frac{K^2}{\omega_a^2} + 2 - 4\zeta^2}{\sqrt{\left(\frac{K^2}{\omega_a^2} + 2 - 4\zeta^2\right)^2 - 4 + 4K^2}} < c_0,$$

  where the second inequality is obtained by observing that, in this case, the function $X(\omega_a)$ is strictly increasing, and by letting $\omega_a \to \infty$.

Second step. For $K \geq 2\zeta$ (cases I and II), from (7) we obtain $\hat{\omega}_c(K,\zeta) \geq 1$. Indeed, the function $\hat{\omega}_c$ is strictly increasing with respect to K and $\hat{\omega}_c(K,\zeta) = 1$ when $K = 2\zeta$. Moreover, from (A5), we have $\tilde{\omega}_c(\omega_a) > \hat{\omega}_c$, $\forall \omega_a > 0$ which gives $\tilde{\omega}_c(\omega_a) > 1, \forall \omega_a > 0$. In this case, using Item (ii) of Proposition 3.3, we have

$$\Delta\bar{\tau}(\omega_a) = \frac{\tan^{-1}\frac{\tilde{\omega}_c(\omega_a)}{\omega_a} + \tan^{-1}\frac{2\zeta\tilde{\omega}_c(\omega_a)}{\tilde{\omega}_c^2(\omega_a)-1}}{\tilde{\omega}_c(\omega_a)}, \tag{A8}$$

of which the derivative with respect to ω_a gives

$$\frac{\mathrm{d}\Delta\bar{\tau}(\omega_a)}{\mathrm{d}\omega_a} = \frac{\mathrm{d}}{\mathrm{d}\omega_a}\left(\frac{\tan^{-1}\frac{\tilde{\omega}_c(\omega_a)}{\omega_a} + \tan^{-1}\frac{2\zeta\tilde{\omega}_c(\omega_a)}{\tilde{\omega}_c^2(\omega_a)-1}}{\tilde{\omega}_c(\omega_a)}\right).$$

Multiplying the above expression by $\tilde{\omega}_c^2(\omega_a)$, we obtain

$$\begin{aligned}
&\tilde{\omega}_c^2(\omega_a)\frac{\mathrm{d}\Delta\bar{\tau}(\omega_a)}{\mathrm{d}\omega_a} \\
&= \frac{\tilde{\omega}_c(\omega_a)\frac{\mathrm{d}}{\mathrm{d}\omega_a}\left(\frac{\tilde{\omega}_c(\omega_a)}{\omega_a}\right)}{1 + \frac{\tilde{\omega}_c^2(\omega_a)}{\omega_a^2}} - \frac{\mathrm{d}\tilde{\omega}_c(\omega_a)}{\mathrm{d}\omega_a}\tan^{-1}\frac{\tilde{\omega}_c(\omega_a)}{\omega_a} \\
&\quad + \frac{\tilde{\omega}_c(\omega_a)\frac{\mathrm{d}}{\mathrm{d}\omega_a}\left(\frac{2\zeta\tilde{\omega}_c(\omega_a)}{\tilde{\omega}_c^2(\omega_a)-1}\right)}{1 + \left(\frac{2\zeta\tilde{\omega}_c(\omega_a)}{\tilde{\omega}_c^2(\omega_a)-1}\right)^2} - \frac{\mathrm{d}\tilde{\omega}_c(\omega_a)}{\mathrm{d}\omega_a}\tan^{-1}\frac{2\zeta\tilde{\omega}_c(\omega_a)}{\tilde{\omega}_c^2(\omega_a)-1}.
\end{aligned} \tag{A9}$$

From (12), we have the following derivatives

$$\frac{\mathrm{d}}{\mathrm{d}\omega_a}\left(\frac{\tilde{\omega}_c(\omega_a)}{\omega_a}\right) = -\frac{\tilde{\omega}_c(\omega_a)}{\omega_a^2} - \frac{K^2X(\omega_a)}{\omega_a^4\tilde{\omega}_c(\omega_a)} \tag{A10}$$

and

$$\begin{aligned}
\frac{\mathrm{d}}{\mathrm{d}\omega_a}\left(\frac{2\zeta\tilde{\omega}_c(\omega_a)}{\tilde{\omega}_c^2(\omega_a)-1}\right) &= \frac{2\zeta K^2(\tilde{\omega}_c^2(\omega_a)+1)X(\omega_a)}{\omega_a^3\tilde{\omega}_c(\omega_a)(\tilde{\omega}_c^2(\omega_a)-1)^2} \\
&= -\frac{2\zeta(\tilde{\omega}_c^2(\omega_a)+1)}{(\tilde{\omega}_c^2(\omega_a)-1)^2}\left(\frac{\mathrm{d}\tilde{\omega}_c(\omega_a)}{\mathrm{d}\omega_a}\right).
\end{aligned} \tag{A11}$$

Replacing (A3), (A10), and (A11) in (A9) and using Item (iii) of Lemma A.1, in the Appendix, we have

$$\begin{aligned}
&\tilde{\omega}_c^2(\omega_a)\frac{\mathrm{d}\Delta\bar{\tau}(\omega_a)}{\mathrm{d}\omega_a} \\
&\leq \frac{-\frac{\tilde{\omega}_c^2(\omega_a)}{\omega_a^2} - \frac{K^2X(\omega_a)}{\omega_a^4}}{1 + \frac{\tilde{\omega}_c^2(\omega_a)}{\omega_a^2}} + \frac{K^2X(\omega_a)}{\omega_a^4}\left(1 + \frac{4\zeta\omega_a\tilde{\omega}_c^2(\omega_a)}{(\tilde{\omega}_c^2(\omega_a)-1)^2}\right) \\
&= \frac{-\frac{\tilde{\omega}_c^2(\omega_a)}{\omega_a^2} + \frac{K^2X(\omega_a)}{\omega_a^4}\left(\frac{\tilde{\omega}_c^2(\omega_a)}{\omega_a^2} + \frac{4\zeta\omega_a^2\tilde{\omega}_c^2(\omega_a) + 4\zeta\tilde{\omega}_c^4(\omega_a)}{\omega_a(\tilde{\omega}_c^2(\omega_a)-1)^2}\right)}{1 + \frac{\tilde{\omega}_c^2(\omega_a)}{\omega_a^2}} \\
&= \frac{\frac{\tilde{\omega}_c^2(\omega_a)}{\omega_a^2}\left(-1 + \frac{K^2X(\omega_a)}{\omega_a^4}\left(1 + \frac{4\zeta\omega_a^3 + 4\zeta\omega_a\tilde{\omega}_c^2(\omega_a)}{(\tilde{\omega}_c^2(\omega_a)-1)^2}\right)\right)}{1 + \frac{\tilde{\omega}_c^2(\omega_a)}{\omega_a^2}}.
\end{aligned}$$

Now consider the term $\frac{\tilde{\omega}_c^2(\omega_a)}{(\tilde{\omega}_c^2(\omega_a)-1)^2}$ in the above expression, we have

$$\frac{\mathrm{d}}{\mathrm{d}\tilde{\omega}_c^2(\omega_a)}\left(\frac{\tilde{\omega}_c^2(\omega_a)}{(\tilde{\omega}_c^2(\omega_a)-1)^2}\right) = \frac{1 - \tilde{\omega}_c^4(\omega_a)}{(\tilde{\omega}_c^2(\omega_a)-1)^4},$$

and since $1 \leq \hat{\omega}_c < \tilde{\omega}_c(\omega_a)$, we can conclude that $\frac{\tilde{\omega}_c^2(\omega_a)}{(\tilde{\omega}_c^2(\omega_a)-1)^2}$ is a strictly decreasing function of $\tilde{\omega}_c(\omega_a)$. Thus $\frac{\tilde{\omega}_c^2(\omega_a)}{(\tilde{\omega}_c^2(\omega_a)-1)^2} < \frac{\hat{\omega}_c^2}{(\hat{\omega}_c^2-1)^2}$, and we obtain

$$\begin{aligned}
&\tilde{\omega}_c^2(\omega_a)\frac{\mathrm{d}\Delta\bar{\tau}(\omega_a)}{\mathrm{d}\omega_a} \\
&< \left(\frac{\frac{\tilde{\omega}_c^2(\omega_a)}{\omega_a^2}}{1 + \frac{\tilde{\omega}_c^2(\omega_a)}{\omega_a^2}}\right)\left(\frac{K^2X(\omega_a)}{\omega_a^4}\left(1 + \frac{4\zeta\omega_a(\hat{\omega}_c^2 + \omega_a^2)}{(\hat{\omega}_c^2-1)^2}\right) - 1\right).
\end{aligned}$$

Using $\frac{\frac{\tilde{\omega}_c^2(\omega_a)}{\omega_a^2}}{1+\frac{\tilde{\omega}_c^2(\omega_a)}{\omega_a^2}} < 1$ gives

$$\tilde{\omega}_c^2(\omega_a)\frac{\mathrm{d}\Delta\bar{\tau}(\omega_a)}{\mathrm{d}\omega_a} < \frac{K^2X(\omega_a)}{\omega_a^4}\left(1 + \frac{4\zeta\omega_a(\hat{\omega}_c^2 + \omega_a^2)}{(\hat{\omega}_c^2-1)^2}\right) - 1.$$

With the upper bounds of $X(\omega_a)$ in (A7), the above inequality yields

- For $K > 1$, (case I)

$$\tilde{\omega}_c^2(\omega_a)\frac{\mathrm{d}\Delta\bar{\tau}(\omega_a)}{\mathrm{d}\omega_a} < \frac{K^2 + c_1\omega_a + c_2\omega_a^3 - \omega_a^4}{\omega_a^4};$$

- For $K \leq 1$, (case II)

$$\tilde{\omega}_c^2(\omega_a)\frac{\mathrm{d}\Delta\bar{\tau}(\omega_a)}{\mathrm{d}\omega_a} < \frac{K^2c_0 + c_1c_0\omega_a + c_2c_0\omega_a^3 - \omega_a^4}{\omega_a^4}.$$

The above expressions can be used to obtain values of $\bar{\omega}_a^*$, from which we have $\frac{\mathrm{d}\Delta\bar{\tau}(\omega_a)}{\mathrm{d}\omega_a} < 0, \forall \omega_a > \bar{\omega}_a^*$. Note, however, to obtain values bounding the set where $\frac{\mathrm{d}\Delta\bar{\tau}(\omega_a)}{\mathrm{d}\omega_a} < 0$, we must find roots of the polynomials $K^2 + c_1\omega_a + c_2\omega_a^3 - \omega_a^4$ and $K^2c_0 + c_1c_0\omega_a + c_2c_0\omega_a^3 - \omega_a^4$. To obtain an

explicit expression for $\bar{\omega}_a^*$, given by the explicit solution of a polynomial of degree 4, we introduce upper-bounds on the right-hand side of the above inequalities by applying the Cauchy–Schwarz inequality either to the terms $c_1\omega_a$ and $c_2\omega_a^3$, or to the terms $c_1c_0\omega_a$ and $c_2c_0\omega_a^3$. The above inequality gives

- For $K > 1$, (case I)

$$\tilde{\omega}_c^2(\omega_a)\frac{\mathrm{d}\Delta\bar{\tau}(\omega_a)}{\mathrm{d}\omega_a} < \frac{K^2 + \frac{c_1^2}{2} + \frac{\omega_a^2}{2} + 2c_2^2\omega_a^2 + \frac{\omega_a^4}{8} - \omega_a^4}{\omega_a^4};$$

- For $K \leq 1$, (case II)

$$\tilde{\omega}_c^2(\omega_a)\frac{\mathrm{d}\Delta\bar{\tau}(\omega_a)}{\mathrm{d}\omega_a} < \frac{K^2c_0 + \frac{c_1^2c_0^2}{2} + \frac{\omega_a^2}{2} + 2c_2^2c_0^2\omega_a^2 + \frac{\omega_a^4}{8} - \omega_a^4}{\omega_a^4}.$$

Again, applying the Cauchy–Schwarz inequality to the term ω_a^2, $c_2^2\omega_a^2$, and $c_2^2c_0^2\omega_a^2$, we obtain

- For $K > 1$, (case I)

$$\tilde{\omega}_c^2(\omega_a)\frac{\mathrm{d}\Delta\bar{\tau}(\omega_a)}{\mathrm{d}\omega_a} < \frac{K^2 + \frac{c_1^2}{2} + \frac{1}{2} + \frac{\omega_a^4}{8} + 8c_2^4 + \frac{\omega_a^4}{8} + \frac{\omega_a^4}{8} - \omega_a^4}{\omega_a^4};$$

- For $K \leq 1$, (case II)

$$\tilde{\omega}_c^2(\omega_a)\frac{\mathrm{d}\Delta\bar{\tau}(\omega_a)}{\mathrm{d}\omega_a} < \frac{K^2c_0 + \frac{c_1^2c_0^2}{2} + \frac{1}{2} + \frac{\omega_a^4}{8} + 8c_2^4c_0^4 + \frac{\omega_a^4}{8} + \frac{\omega_a^4}{8} - \omega_a^4}{\omega_a^4}.$$

Thus, from the roots to the right-hand side of the above two inequalities, we get directly the explicit upper bound $\bar{\omega}_a^*$ stated in the theorem for which $\frac{\mathrm{d}\Delta\bar{\tau}(\omega_a)}{\mathrm{d}\omega_a}$ is negative for all $\omega_a \geq \bar{\omega}_a^*$.

Third step. The argument invoked at the beginning of the *Second step*, for $K < 2\zeta$ (cases III and IV), gives $\hat{\omega}_c < 1$. From (12), we can show that $\tilde{\omega}_c(\omega_a) < 1$ if and only if $\omega_a > \frac{K}{\sqrt{4\zeta^2 - K^2}}$. Then, in this case, the set $\{\omega_a \mid \tilde{\omega}_c(\omega_a) < 1\}$ is not empty. Therefore, given any pair (K, ζ) in the set III $\cup$ IV, from Item (iv) of Lemma A.1, we have, for all $\omega_a > 0$,

$$\max_{\tilde{\omega}_c(\omega_a)>1}\left\{\tan^{-1}\frac{2\zeta\tilde{\omega}_c(\omega_a)}{\tilde{\omega}_c^2(\omega_a) - 1}\right\} < \frac{\pi}{2} < \min_{\tilde{\omega}_c(\omega_a)<1}\left\{-\tan^{-1}\frac{2\zeta\tilde{\omega}_c(\omega_a)}{1 - \tilde{\omega}_c^2(\omega_a)} + \pi\right\}. \tag{A12}$$

Moreover, since $\frac{\tan^{-1}\frac{\tilde{\omega}_c(\omega_a)}{\omega_a}}{\tilde{\omega}_c(\omega_a)}$ is a decreasing function with respect to $\tilde{\omega}_c(\omega_a)$, we also have, for all $\omega_a > 0$,

$$\max_{\tilde{\omega}_c(\omega_a)>1}\left\{\frac{\tan^{-1}\frac{\tilde{\omega}_c(\omega_a)}{\omega_a}}{\tilde{\omega}_c(\omega_a)}\right\} < \min_{\tilde{\omega}_c(\omega_a)<1}\left\{\frac{\tan^{-1}\frac{\tilde{\omega}_c(\omega_a)}{\omega_a}}{\tilde{\omega}_c(\omega_a)}\right\}. \tag{A13}$$

Using (A12), (A13), and Proposition 3.3.(ii), we can show that, for all $\omega_a > 0$, the delay margin in the case where $\tilde{\omega}_c(\omega_a) < 1$ (which is only possible in the cases III and IV) is larger than the delay margin in the case where $\tilde{\omega}_c(\omega_a) \geq 1$. For this reason, and using the fact that the set $\{\omega_a \mid \tilde{\omega}_c(\omega_a) > 1\}$ is not empty, we consider the case where $\tilde{\omega}_c(\omega_a) < 1$ to maximise the delay margin. In this case, from (11), we have

$$\Delta\bar{\tau}(\omega_a) = \frac{\tan^{-1}\frac{\tilde{\omega}_c(\omega_a)}{\omega_a} - \tan^{-1}\frac{2\zeta\tilde{\omega}_c(\omega_a)}{1-\tilde{\omega}_c^2(\omega_a)} + \pi}{\tilde{\omega}_c(\omega_a)}.$$

From the above expression, we then follow closely the developments starting from (A8) in the above *Second step*, which we omit for brevity, to arrive at the following expressions

- For $K > 1$, (case III)

$$\tilde{\omega}_c^2(\omega_a)\frac{\mathrm{d}\Delta\bar{\tau}(\omega_a)}{\mathrm{d}\omega_a} < \frac{4 + 4K^2 + 2(c_1^2 + c_3^2) + 32(c_2^4 + c_4^4) - \omega_a^4}{4\omega_a^4};$$

- For $K \leq 1$ and $2\zeta\sqrt{1-\zeta^2} < K$, (case IV)

$$\tilde{\omega}_c^2(\omega_a)\frac{\mathrm{d}\Delta\bar{\tau}(\omega_a)}{\mathrm{d}\omega_a} < \frac{4 + 4K^2c_0 + 2(c_1^2 + c_3^2)c_0^2 + 32(c_2^4 + c_4^4)c_0^4 - \omega_a^4}{4\omega_a^4}.$$

Finally, from the right-hand side of the last inequality, we get directly the explicit upper bound $\bar{\omega}_a^*$ stated in the theorem. ■

We provide here the following lemma, which is used in the proof, given below, of Theorem 3.5.

Lemma A.2: *For any scalar $K > 0$, let the function $Z : \mathbb{R}_{>0} \times \mathbb{R}_{>0} \to \mathbb{R}_{>0}$ be defined as*

$$Z(\omega_a, K) = Y(\omega_a, K)\tan^{-1}\frac{\bar{\omega}_c(\omega_a, K)}{\omega_a} - \frac{\bar{\omega}_c^2(\omega_a, K) + \frac{\bar{\omega}_c(\omega_a,K)}{\omega_a}Y(\omega_a, K)}{1 + \frac{\bar{\omega}_c^2(\omega_a,K)}{\omega_a^2}}, \tag{A14}$$

where

$$\bar{\omega}_c(\omega_a, K) = \sqrt{\frac{\frac{K^2}{\omega_a^2} + \sqrt{\frac{K^4}{\omega_a^4} + 4K^2}}{2}} \quad \textit{and} \quad Y(\omega_a, K) = \frac{K^2\bar{\omega}_c(\omega_a, K)}{\omega_a\sqrt{\frac{K^4}{\omega_a^4} + 4K^2}}. \tag{A15}$$

Moreover, let the function $\psi : \mathbb{R}_{>0} \to \mathbb{R}_{>0}$ be defined as

$$\psi(\vartheta) = \frac{\beta(\vartheta)}{\vartheta\gamma(\vartheta)}\tan^{-1}\frac{\beta(\vartheta)}{\vartheta} - \frac{\beta^2(\vartheta) + \frac{\beta^2(\vartheta)}{\vartheta^2\gamma(\vartheta)}}{1 + \frac{\beta^2(\vartheta)}{\vartheta^2}}, \tag{A16}$$

where

$$\beta(\vartheta) = \sqrt{\frac{\frac{1}{\vartheta^2} + \sqrt{\frac{1}{\vartheta^4} + 4}}{2}} \quad \textit{and} \quad \gamma(\vartheta) = \sqrt{\frac{1}{\vartheta^4} + 4}. \tag{A17}$$

The functions Z and ψ have the following properties:

(i) *There exists a unique solution $\alpha > 0$ of the implicit equation $\psi(\vartheta) = 0$.*
(ii) *For any $\eta \in \mathbb{R}_{>0}$ and $K \in \mathbb{R}_{>0}$, we have $Z(\alpha\sqrt{K}\eta, K) = \psi(\alpha\eta)$.*
(iii) *For any fixed value of $K > 0$, the equation $Z(\omega_a, K) = 0$ admits a unique solution $\omega_a = \alpha\sqrt{K}$.*

Proof: *Item (i).* Let us first show that $\frac{\mathrm{d}\psi(\vartheta)}{\mathrm{d}\vartheta} < 0$. The derivative of ψ with respect to ϑ is given by

$$\frac{\mathrm{d}\psi(\vartheta)}{\mathrm{d}\vartheta} = \frac{\mathrm{d}}{\mathrm{d}\omega_a}\left(\frac{\beta(\vartheta)}{\vartheta\gamma(\vartheta)}\right)\tan^{-1}\frac{\beta(\vartheta)}{\vartheta} - \frac{\frac{\beta(\vartheta)}{\vartheta}\frac{\mathrm{d}}{\mathrm{d}\vartheta}\left(\frac{\beta(\vartheta)}{\vartheta\gamma(\vartheta)}\right)}{1 + \frac{\beta^2(\vartheta)}{\vartheta^2}} - \frac{2\beta(\vartheta)\frac{\mathrm{d}\beta(\vartheta)}{\mathrm{d}\vartheta}}{1 + \frac{\beta^2(\vartheta)}{\vartheta^2}} + \frac{\beta^2(\vartheta)\frac{\mathrm{d}}{\mathrm{d}\vartheta}\left(\frac{\beta^2(\vartheta)}{\vartheta^2}\right)}{\left(1 + \frac{\beta^2(\vartheta)}{\vartheta^2}\right)^2} + \frac{\frac{\beta^2(\vartheta)}{\vartheta^2\gamma(\vartheta)}\frac{\mathrm{d}}{\mathrm{d}\vartheta}\left(\frac{\beta^2(\vartheta)}{\vartheta^2}\right)}{\left(1 + \frac{\beta^2(\vartheta)}{\vartheta^2}\right)^2}.$$

From (A17), we have $\frac{\mathrm{d}}{\mathrm{d}\vartheta}\left(\frac{\beta(\vartheta)}{\vartheta\gamma(\vartheta)}\right) < 0$ for all $\vartheta > 0$. Using Lemma A.1.(iii), the above expression is upper-bounded by

$$\frac{\mathrm{d}\psi(\vartheta)}{\mathrm{d}\vartheta} \leq -\frac{2\beta(\vartheta)\frac{\mathrm{d}\beta(\vartheta)}{\mathrm{d}\vartheta}}{1 + \frac{\beta^2(\vartheta)}{\vartheta^2}} + \frac{\beta^2(\vartheta)\frac{\mathrm{d}}{\mathrm{d}\vartheta}\left(\frac{\beta^2(\vartheta)}{\vartheta^2}\right)}{\left(1 + \frac{\beta^2(\vartheta)}{\vartheta^2}\right)^2} + \frac{\frac{\beta^2(\vartheta)}{\vartheta^2\gamma(\vartheta)}\frac{\mathrm{d}}{\mathrm{d}\vartheta}\left(\frac{\beta^2(\vartheta)}{\vartheta^2}\right)}{\left(1 + \frac{\beta^2(\vartheta)}{\vartheta^2}\right)^2}. \tag{A18}$$

From (A17), we have

$$\frac{\mathrm{d}\beta(\vartheta)}{\mathrm{d}\vartheta} = -\frac{1}{\vartheta^3\beta(\vartheta)}\left(\frac{\frac{1}{\vartheta^2} + \sqrt{\frac{1}{\vartheta^4} + 4}}{2\sqrt{\frac{1}{\vartheta^4} + 4}}\right).$$

Using the fact that $0 < \frac{\frac{1}{\vartheta^2} + \sqrt{\frac{1}{\vartheta^4} + 4}}{2\sqrt{\frac{1}{\vartheta^4} + 4}} \leq 1$ and since $\frac{1}{\vartheta^3\beta(\vartheta)} > 0$, the above equation gives

$$-\frac{1}{\vartheta^3\beta(\vartheta)} \leq \frac{\mathrm{d}\beta(\vartheta)}{\mathrm{d}\vartheta} < 0. \tag{A19}$$

Using (A19), we have

$$\frac{\mathrm{d}}{\mathrm{d}\vartheta}\left(\frac{\beta^2(\vartheta)}{\vartheta^2}\right)=\frac{2\beta(\vartheta)}{\vartheta^2}\left(\frac{\mathrm{d}\beta(\vartheta)}{\mathrm{d}\vartheta}-\frac{\beta(\vartheta)}{\vartheta}\right)<0. \tag{A20}$$

Then, since the last term in (A18) is negative, it gives

$$\begin{aligned}\frac{\mathrm{d}\psi(\vartheta)}{\mathrm{d}\vartheta} &< \frac{-2\beta(\vartheta)\left(1+\frac{\beta^2(\vartheta)}{\vartheta^2}\right)\frac{\mathrm{d}\beta(\vartheta)}{\mathrm{d}\vartheta}+\beta^2(\vartheta)\frac{\mathrm{d}}{\mathrm{d}\vartheta}\left(\frac{\beta^2(\vartheta)}{\vartheta^2}\right)}{\left(1+\frac{\beta^2(\vartheta)}{\vartheta^2}\right)^2}\\ \text{(A20)}&=\frac{-2\beta(\vartheta)\frac{\mathrm{d}\beta(\vartheta)}{\mathrm{d}\vartheta}-\frac{2\beta^3(\vartheta)}{\vartheta^2}\frac{\mathrm{d}\beta(\vartheta)}{\mathrm{d}\vartheta}+\frac{2\beta^3(\vartheta)}{\vartheta^2}\left(\frac{\mathrm{d}\beta(\vartheta)}{\mathrm{d}\vartheta}-\frac{\beta(\vartheta)}{\vartheta}\right)}{\left(1+\frac{\beta^2(\vartheta)}{\vartheta^2}\right)^2}\\ &=\frac{-2\beta(\vartheta)\frac{\mathrm{d}\beta(\vartheta)}{\mathrm{d}\vartheta}-\frac{2\beta^4(\vartheta)}{\vartheta^3}}{\left(1+\frac{\beta^2(\vartheta)}{\vartheta^2}\right)^2}\\ (A19)&<\frac{\frac{2}{\vartheta^3}-\frac{2\beta^4(\vartheta)}{\vartheta^3}}{\left(1+\frac{\beta^2(\vartheta)}{\vartheta^2}\right)^2}.\end{aligned}$$

Using the fact that, from (A17), we have $\beta(\vartheta)>1$, the above inequality gives

$$\frac{\mathrm{d}\psi(\vartheta)}{\mathrm{d}\vartheta}<0.$$

Therefore, the function $\psi(\vartheta)$ is a strictly decreasing function with respect to ϑ.

To obtain existence and uniqueness of a solution to $\psi(\vartheta)=0$, we show that $\lim_{\vartheta\to 0}\psi(\vartheta)>0$ and $\lim_{\vartheta\to+\infty}\psi(\vartheta)<0$. From (A17), we have

$$\lim_{\vartheta\to 0}\frac{\beta(\vartheta)}{\frac{1}{\vartheta}}=1 \tag{A21}$$

and

$$\lim_{\vartheta\to 0}\frac{\gamma(\vartheta)}{\frac{1}{\vartheta^2}}=1. \tag{A22}$$

We also have

$$\lim_{\vartheta\to+\infty}\beta(\vartheta)=1 \tag{A23}$$

and

$$\lim_{\vartheta\to+\infty}\gamma(\vartheta)=2. \tag{A24}$$

Then, let us consider the expression of $\psi(\vartheta)$ in (A16). Using (A21) and (A22), namely by replacing $\beta(\vartheta)$ by $\frac{1}{\vartheta}$ and replacing $\gamma(\vartheta)$ by $\frac{1}{\vartheta^2}$, we obtain

$$\lim_{\vartheta\to 0}\psi(\vartheta)=\frac{\pi}{2}-\lim_{\vartheta\to 0}\frac{\beta^2(\vartheta)+\frac{\beta^2(\vartheta)}{\vartheta^2\gamma(\vartheta)}}{1+\frac{\beta^2(\vartheta)}{\vartheta^2}}=\frac{\pi}{2}.$$

And, using (A23) and (A24), namely by setting $\beta(\vartheta)=1$ and $\gamma(\vartheta)=2$, we obtain

$$\lim_{\vartheta\to+\infty}\psi(\vartheta)=0-\lim_{\vartheta\to+\infty}\frac{\beta^2(\vartheta)+\frac{\beta^2(\vartheta)}{\vartheta^2\gamma(\vartheta)}}{1+\frac{\beta^2(\vartheta)}{\vartheta^2}}=-1.$$

Therefore, since $\psi(\vartheta)$ is positive near zero, negative at $+\infty$, and it is continuous and a strictly decreasing function with respect to ϑ, then, the solution of $\psi(\vartheta)=0$ exists and is unique.

Item (ii). To show that, for any $\eta\in\mathbb{R}_{>0}$ and $K\in\mathbb{R}_{>0}$, we have $Z(\alpha\sqrt{K}\eta,K)=\psi(\alpha\eta)$, consider (A14) and (A15) to obtain

$$\begin{aligned}Z(\alpha\sqrt{K}\eta,K)&=Y(\alpha\sqrt{K}\eta,K)\tan^{-1}\frac{\bar{\omega}_c(\alpha\sqrt{K}\eta,K)}{\alpha\sqrt{K}\eta}\\ &\quad-\frac{\bar{\omega}_c^2(\alpha\sqrt{K}\eta,K)+\frac{\bar{\omega}_c(\alpha\sqrt{K}\eta,K)}{\alpha\sqrt{K}\eta}Y(\alpha\sqrt{K}\eta,K)}{1+\frac{\bar{\omega}_c^2(\alpha\sqrt{K}\eta,K)}{\alpha^2K\eta^2}},\end{aligned}$$

$$\bar{\omega}_c(\alpha\sqrt{K}\eta,K)=\sqrt{\frac{\frac{K^2}{\alpha^2K\eta^2}+\sqrt{\frac{K^4}{\alpha^4K^2\eta^4}+4K^2}}{2}}$$

$$=\sqrt{K}\beta(\alpha\eta),$$

and

$$\begin{aligned}Y(\alpha\sqrt{K}\eta,K)&=\frac{K^2\bar{\omega}_c(\alpha\sqrt{K}\eta)}{\alpha\sqrt{K}\eta\sqrt{\frac{K^4}{\alpha^4K^2\eta^4}+4K^2}}\\ &=\frac{K^2\sqrt{K}\beta(\alpha\eta)}{\alpha\sqrt{K}\eta K\sqrt{\frac{1}{\alpha^4\eta^4}+4}}\\ &=\frac{K\beta(\alpha\eta)}{\alpha\eta\gamma(\alpha\eta)}.\end{aligned}$$

Replacing the expression of $\bar{\omega}_c(\alpha\sqrt{K}\eta,K)$ and $Y(\alpha\sqrt{K}\eta,K)$ in the expression of $Z(\alpha\sqrt{K}\eta,K)$ and simplifying with K, we thus have, for any $\eta\in\mathbb{R}_{>0}$ and $K\in\mathbb{R}_{>0}$, $Z(\alpha\sqrt{K}\eta,K)=\psi(\alpha\eta)$, where ψ is given by (A16).

Item (iii). For a fixed value of K, suppose that $\omega_a=x^*$ is a solution to $Z(\omega_a,K)=0$. From *Item* (ii), we have $Z(\alpha\sqrt{K}\eta,K)=\psi(\alpha\eta)$.

Take $\eta=\frac{x^*}{\alpha\sqrt{K}}$, we obtain

$$\psi\left(\frac{x^*}{\sqrt{K}}\right)=0$$

since by assumption $Z(x^*,K)=0$. Then, from *Item* (i), we must have

$$\frac{x^*}{\sqrt{K}}=\alpha.$$

Therefore, $\omega_a=x^*=\alpha\sqrt{K}$ is the unique solution of $Z(\omega_a,K)=0$. ■

Proof of Theorem 3.5: The goal in the steps detailed below is to obtain the asymptote of ω_a^*, the value of ω_a yielding the optimal delay margin $\Delta\bar{\tau}(\omega_a)$, as K tends to $+\infty$.

First step. For any fixed value of $\zeta>0$, using the results of Theorem 3.4 (case I), there exist a scalar $\delta>0$, where $\omega_a^*(K,\zeta)<\delta\sqrt{K}$ as K tends to $+\infty$. Then, from (12), for any $\omega_a<\delta\sqrt{K}$ we have

$$\lim_{K\to+\infty}\frac{\tilde{\omega}_c(\omega_a,K,\zeta)}{\sqrt{\frac{\frac{K^2}{\omega_a^2}+\sqrt{\frac{K^4}{\omega_a^4}+4K^2}}{2}}}=1. \tag{A25}$$

We thus have that $\lim_{K\to+\infty}\tilde{\omega}_c(\omega_a)=+\infty$. Using the argument invoked at the beginning of *Second step* in the proof of Theorem 3.4, for $K\geq 2\zeta$, we have $\tilde{\omega}_c(\omega_a)>1$. In this case, from (11), we have

$$\Delta\bar{\tau}(\omega_a)=\frac{\tan^{-1}\frac{\tilde{\omega}_c(\omega_a)}{\omega_a}+\tan^{-1}\frac{2\zeta\tilde{\omega}_c(\omega_a)}{\tilde{\omega}_c^2(\omega_a)-1}}{\tilde{\omega}_c(\omega_a)}.$$

of which the derivative with respect to ω_a gives

$$\frac{\mathrm{d}\Delta\bar{\tau}(\omega_a)}{\mathrm{d}\omega_a}=\frac{\mathrm{d}}{\mathrm{d}\omega_a}\left(\frac{\tan^{-1}\frac{\tilde{\omega}_c(\omega_a)}{\omega_a}+\tan^{-1}\frac{2\zeta\tilde{\omega}_c(\omega_a)}{\tilde{\omega}_c^2(\omega_a)-1}}{\tilde{\omega}_c(\omega_a)}\right).$$

Multiplying the above expression by $\tilde{\omega}_c^2(\omega_a)$, we obtain

$$\begin{aligned}&\tilde{\omega}_c^2(\omega_a)\frac{\mathrm{d}\Delta\bar{\tau}(\omega_a)}{\mathrm{d}\omega_a}\\ &=\frac{\tilde{\omega}_c(\omega_a)\frac{\mathrm{d}}{\mathrm{d}\omega_a}\left(\frac{\tilde{\omega}_c(\omega_a)}{\omega_a}\right)}{1+\frac{\tilde{\omega}_c^2(\omega_a)}{\omega_a^2}}-\frac{\mathrm{d}\tilde{\omega}_c(\omega_a)}{\mathrm{d}\omega_a}\tan^{-1}\frac{\tilde{\omega}_c(\omega_a)}{\omega_a}\\ &\quad+\frac{\tilde{\omega}_c(\omega_a)\frac{\mathrm{d}}{\mathrm{d}\omega_a}\left(\frac{2\zeta\tilde{\omega}_c(\omega_a)}{\tilde{\omega}_c^2(\omega_a)-1}\right)}{1+\left(\frac{2\zeta\tilde{\omega}_c(\omega_a)}{\tilde{\omega}_c^2(\omega_a)-1}\right)^2}-\frac{\mathrm{d}\tilde{\omega}_c(\omega_a)}{\mathrm{d}\omega_a}\tan^{-1}\frac{2\zeta\tilde{\omega}_c(\omega_a)}{\tilde{\omega}_c^2(\omega_a)-1}.\end{aligned} \tag{A26}$$

From (A3), (A4), (A10), and (A11), we can obtain

$$\lim_{K\to+\infty}\frac{\frac{\mathrm{d}}{\mathrm{d}\omega_a}\left(\frac{\tilde{\omega}_c(\omega_a)}{\omega_a}\right)}{-\frac{\tilde{\omega}_c(\omega_a)}{\omega_a^2}-\frac{K^2\tilde{\omega}_c(\omega_a)}{\omega_a^4\sqrt{\frac{K^4}{\omega_a^4}+4K^2}}}=1, \tag{A27}$$

$$\lim_{K\to+\infty} \frac{\frac{\mathrm{d}\tilde{\omega}_c(\omega_a)}{\mathrm{d}\omega_a}}{-\frac{K^2\tilde{\omega}_c(\omega_a)}{\omega_a^3\sqrt{\frac{K^4}{\omega_a^4}+4K^2}}} = 1, \tag{A28}$$

and

$$\lim_{K\to+\infty} \frac{\frac{\mathrm{d}}{\mathrm{d}\omega_a}\left(\frac{2\zeta\tilde{\omega}_c(\omega_a)}{\tilde{\omega}_c^2(\omega_a)-1}\right)}{\frac{2\zeta K^2}{\omega_a^3\tilde{\omega}_c(\omega_a)\sqrt{\frac{K^4}{\omega_a^4}+4K^2}}} = 1.$$

Now, using the above three limits and since $\lim_{K\to+\infty} \frac{2\zeta\tilde{\omega}_c(\omega_a)}{\tilde{\omega}_c^2(\omega_a)-1} = 0$, we have

$$\lim_{K\to+\infty} \frac{\frac{\tilde{\omega}_c(\omega_a)\frac{\mathrm{d}}{\mathrm{d}\omega_a}\left(\frac{2\zeta\tilde{\omega}_c(\omega_a)}{\tilde{\omega}_c^2(\omega_a)-1}\right)}{1+\left(\frac{2\zeta\tilde{\omega}_c(\omega_a)}{\tilde{\omega}_c^2(\omega_a)-1}\right)^2} - \frac{\mathrm{d}\tilde{\omega}_c(\omega_a)}{\mathrm{d}\omega_a}\tan^{-1}\frac{2\zeta\tilde{\omega}_c(\omega_a)}{\tilde{\omega}_c^2(\omega_a)-1}}{\frac{\tilde{\omega}_c(\omega_a)\frac{\mathrm{d}}{\mathrm{d}\omega_a}\left(\frac{\tilde{\omega}_c(\omega_a)}{\omega_a}\right)}{1+\frac{\tilde{\omega}_c^2(\omega_a)}{\omega_a^2}} - \frac{\mathrm{d}\tilde{\omega}_c(\omega_a)}{\mathrm{d}\omega_a}\tan^{-1}\frac{\tilde{\omega}_c(\omega_a)}{\omega_a}} = 0.$$

Therefore, from (A26), we obtain the following expression:

$$\lim_{K\to+\infty} \frac{\tilde{\omega}_c^2(\omega_a)\frac{\mathrm{d}\Delta\bar{\tau}(\omega_a)}{\mathrm{d}\omega_a}}{\frac{\tilde{\omega}_c(\omega_a)\frac{\mathrm{d}}{\mathrm{d}\omega_a}\left(\frac{\tilde{\omega}_c(\omega_a)}{\omega_a}\right)}{1+\frac{\tilde{\omega}_c^2(\omega_a)}{\omega_a^2}} - \frac{\mathrm{d}\tilde{\omega}_c(\omega_a)}{\mathrm{d}\omega_a}\tan^{-1}\frac{\tilde{\omega}_c(\omega_a)}{\omega_a}} = 1.$$

Using (A27) and (A28), namely, replacing $\frac{\mathrm{d}}{\mathrm{d}\omega_a}(\frac{\tilde{\omega}_c(\omega_a)}{\omega_a})$ by $-\frac{\tilde{\omega}_c(\omega_a)}{\omega_a^2} - \frac{K^2\tilde{\omega}_c(\omega_a)}{\omega_a^4\sqrt{\frac{K^4}{\omega_a^4}+4K^2}}$ and replacing $\frac{\mathrm{d}\tilde{\omega}_c(\omega_a)}{\mathrm{d}\omega_a}$ by $-\frac{K^2\tilde{\omega}_c(\omega_a)}{\omega_a^3\sqrt{\frac{K^4}{\omega_a^4}+4K^2}}$ in the above equation and multiplying by ω_a^2, we obtain

$$\lim_{K\to+\infty} \frac{\omega_a^2\tilde{\omega}_c^2(\omega_a)\frac{\mathrm{d}\Delta\bar{\tau}(\omega_a)}{\mathrm{d}\omega_a}}{Z(\omega_a,K)} = 1, \quad \forall\,\omega_a > 0, \tag{A29}$$

where, using (A25), $Z(\omega_a, K)$ is given by (A14) in Lemma A.2.

Second step. Using Lemma A.2, the optimal solution $\omega_a^*(K,\zeta)$ exists and is unique. Now, consider a function $\varphi : \mathbb{R}_{>0} \to \mathbb{R}_{>0}$, such that $\varphi(K) < \delta\sqrt{K}$ satisfying

$$\lim_{K\to+\infty} \frac{\omega_a^*(K,\zeta)}{\varphi(K)} = 1. \tag{A30}$$

Setting $\omega_a = \varphi(K)$, and from the fact that ω_a^* yields the maximum delay margin, namely, for all K, $\frac{\mathrm{d}\Delta\bar{\tau}}{\mathrm{d}\omega_a}(\omega_a^*(K,\zeta)) = 0$, thus $(\omega_a^*(K,\zeta)\,\tilde{\omega}_c(\omega_a^*(K,\zeta)))^2\frac{\mathrm{d}\Delta\bar{\tau}}{\mathrm{d}\omega_a}(\omega_a^*(K,\zeta)) = 0$. Hence, using the above equivalence between $\omega_a^*(K,\zeta)$ and $\varphi(K)$, we have

$$\lim_{K\to+\infty} \varphi^2(K)\tilde{\omega}_c^2(\varphi(K))\frac{\mathrm{d}\Delta\bar{\tau}}{\mathrm{d}\omega_a}(\varphi(K)) = 0.$$

Therefore, from (A29), we must have

$$\lim_{K\to+\infty} Z(\varphi(K),K) = 0. \tag{A31}$$

Third step. Consider the unique solution $\alpha > 0$ of (A16) and let us rewrite $\varphi(K)$ as

$$\varphi(K) = \alpha\sqrt{K}\eta(K),$$

where $\eta : \mathbb{R}_{>0} \to \mathbb{R}_{>0}$. Let us suppose that (A31) holds and that $\lim_{K\to+\infty}\frac{\alpha\sqrt{K}}{\varphi(K)} \neq 1$, which from the above equation is equivalent to $\lim_{K\to+\infty}\eta(K) \neq 1$. Using Lemma A.2, we have $Z(\alpha\sqrt{K}\eta(K),K) = \psi(\alpha\eta(K))$. Since the unique solution of equation $\psi(\vartheta) = 0$ is $\vartheta = \alpha$ we have that

$$\psi\left(\alpha\lim_{K\to+\infty}\eta(K)\right) \neq 0.$$

The continuity of ψ thus implies that

$$\lim_{K\to+\infty}\psi(\alpha\eta(K)) \neq 0,$$

which from Lemma A.2.(ii) implies

$$\lim_{K\to+\infty} Z(\varphi(K),K) \neq 0,$$

that is, (A31) can not hold, leading to a contradiction. We thus conclude that

$$\lim_{K\to+\infty}\frac{\alpha\sqrt{K}}{\varphi(K)} = 1$$

and, from (A30), we have

$$\lim_{K\to+\infty}\frac{\omega_a^*(K,\zeta)}{\alpha\sqrt{K}} = 1.$$

■